energies

MDPI

Review

Review of the Coupled System of Solar and Air Source Heat Pump

Xin Meng [1,2,*], Xin Zhou [2] and Zhenyu Li [2]

[1] School of Power and Energy Engineering, Xi'an Jiaotong University, Xi'an 710049, China
[2] School of Mechanical Engineering, Shaanxi University of Technology, Hanzhong 723001, China; xinzhou0958@163.com (X.Z.); 18291780938@163.com (Z.L.)
* Correspondence: xinmeng@snut.edu.cn

Abstract: The coupled operation of solar energy and air source heat pump (ASHP) can effectively solve the intermittent problem of solar energy systems running alone and the problem of performance degradation of ASHP systems running alone in winter. The coupled system of solar energy and ASHP can be divided into direct expansion type and indirect expansion type according to the structure form, and the indirect expansion type can be divided into series type, parallel type, and hybrid type. Various architectural forms of the solar-air source heat pump coupled system (S–ASHP) have achieved enhanced energy efficiency by means of a series of strategies, including the optimization of collectors, the refinement of evaporator structures, and the regulation of the temperature within hot water storage tanks. Choosing the appropriate architecture needs to comprehensively consider factors such as the external environment and load demand. In this paper, a variety of S–ASHP are summarized in order to provide some guidance for the future application of S–ASHP systems in the field of heating.

Keywords: solar energy; air source heat pump; coupled system

check for updates

Citation: Meng, X.; Zhou, X.; Li, Z. Review of the Coupled System of Solar and Air Source Heat Pump. *Energies* **2024**, *17*, 6045. https://doi.org/10.3390/en17236045

Academic Editor: Ioan Sarbu

Received: 17 October 2024
Revised: 27 November 2024
Accepted: 28 November 2024
Published: 1 December 2024

Copyright: © 2024 by the authors. Licensee MDPI, Basel, Switzerland. This article is an open access article distributed under the terms and conditions of the Creative Commons Attribution (CC BY) license (https://creativecommons.org/licenses/by/4.0/).

1. Introduction

With the widespread use of fossil fuels in countries around the world, global warming is already about 1.0 °C above pre-industrial levels. Given the current growth rate of carbon dioxide emissions, it is expected to rise to more than 1.5 °C between 2030 and 2052 [1]. In response to global climate change, energy transformation has become a historical necessity for the continuous progress of human civilization. In order to achieve the "two–carbon" goal, China will take a series of major measures, including promoting the use of renewable energy and reducing the use of fossil fuels, especially coal [2,3]. In order to cope with the energy crisis and environmental challenges, the use of renewable energy to replace fossil fuels has become the focus of countries around the world. In order to reduce China's dependence on fossil fuels, the transformation of the energy structure has been carried out, and the proportion of renewable energy in the whole fuel structure has been increased. By 2030, China plans to make the proportion of renewable energy reach 16%. By 2050, the proportion of renewable energy is 60%, and the proportion of renewable electricity is 86% [4]. Palestine has considerable potential in the field of renewable energy. In order to meet people's demand for electricity in the future, the growth rate of renewable energy should be maintained at about 5–10% per year [5]. In order to reduce carbon emissions, the UK will vigorously promote the use of wind and solar energy. It is anticipated that by 2030, 180 TWh of electricity will be generated from wind energy and 23 TWh from solar energy, respectively. This represents a 2.2-fold increase compared to 2023 [6]. In Western Australia, more than 35% of home users already use solar systems, and the government has set a goal of net zero emissions by 2050 [7]. Many other countries are also using renewable energy to replace fossil fuels.

Solar energy is an inexhaustible clean energy with great application potential. Solar energy mainly has two application modes, solar thermal utilization and solar photovoltaic power generation. Compared with traditional energy sources, solar energy is generated by nuclear fusion reactions inside the sun. As long as the sun exists, solar energy can be continuously utilized. Solar energy is widely distributed and can be obtained almost anywhere, without geographical restrictions. Solar energy does not produce any pollutants and greenhouse gasses in the process of utilization, which is environmentally friendly. Solar collectors (SC) can not only meet the daily heat load but also reduce the use of fossil fuels [8]. At the time of economic development, the demand for production and domestic electricity has increased, and solar power generation technology has received increasing attention [9]. However, due to the influence of seasons, weather, and other factors, the supply of solar energy is intermittent and unstable [10].

An air source heat pump (ASHP) is a kind of heat pump system with air as a heat source. It works according to the principle of the inverse Carnot cycle. The heat pump can convert the low-grade heat energy in the air into high-grade heat energy by consuming only a small amount of electric energy, so as to realize the functions of heating and supplying hot water. Compared with traditional heating modes, such as electric heating, gas boiler heating, and coal-fired boiler heating, ASHP has a significant energy-saving effect. During operation, the ASHP will not produce any pollutants or greenhouse gasses, very friendly to the environment. Moreover, the ASHP does not need to install a complex pipeline system and a boiler room. It is only necessary to install a heat pump unit and a water tank outdoors. The installation process is convenient and fast. However, the ASHP also has some shortcomings. In the low-temperature environment, the performance of the ASHP will be significantly reduced, and the heating effect will be poor [11,12]. The operation noise of ASHP is large, which has a certain impact on the surrounding environment.

In order to break through the limitations of solar intermittence and instability, and improve the efficiency of solar energy utilization and the performance and stability of ASHP, some scholars have begun to study the method of integrating solar energy and ASHP technology. Solar–air source heat pump coupling system (S–ASHP) is a new energy system that combines SC and ASHP units to provide heating and hot water for buildings. The system gives full play to the respective advantages of solar energy and ASHP, effectively overcomes their respective shortcomings, achieves the complementary use of energy, and enhances the overall performance and stability of the system. With the continuous progress of technology and the continuous decline of cost, the research and application of the S–ASHP system are developing rapidly. Kim et al. [13] proposed hybrid solar collector consists of a solar thermal receiver and an air source receiver. In the absence of solar radiation, the air source receiver can work in the air heat exchanger mode with a fan. The solar-assisted heat pump of this hybrid solar collector exhibits excellent performance, with annual operating hours of up to 7036 h. Abbasi et al. [14] study on the effect of solar radiation and ambient air temperature on the thermodynamic performance of direct-expansion solar-assisted heat pump (DX-SAHP) is carried out. The results show that when the ambient temperature rises or the solar radiation level rises, the COP value also shows an upward trend. The S–ASHP system has different forms, which can be divided into two categories, direct expansion and indirect expansion. Shi et al. [15] reviewed the direct expansion solar–air source heat pump coupled (DX–S-ASHP) system. The results show that the combination of SC/evaporator with photovoltaic cells, phase change thermal storage materials (PCM), heat pipes, and other advanced technologies can improve the performance of the system under the same climatic conditions. At the same time, researchers have also conducted in-depth and comprehensive research on indirect expansion. Zhou et al. [16] comprehensively reviewed the indirect expansion solar–air source heat pump coupled system (IDX–S-ASHP), mainly from the aspects of component structure, heat storage technology, operation mode, and control strategy, and summarized its advantages and disadvantages. At present, the S–ASHP system has been widely used in many buildings at home and abroad and has achieved considerable economic and environmental benefits.

This research review is intended to comprehensively arrange the research status of the S–ASHP system. This paper will arrange and analyze the research results of coupling systems with different architectures (mainly including DX–S-ASHP and IDX–S-ASHP), so as to clarify the research status and development trend of the system. Furthermore, it provides a reference for the subsequent coupling mode improvement of the S-ASHP system, system adaptability, and performance optimization research in different external environments. In addition, by summarizing the performance characteristics and optimization design methods of coupled systems with different configurations, it can provide technical support and reference for practical engineering applications, and finally achieve the purpose of improving the efficiency and stability of the system.

2. Solar–Air Source Heat Pump Coupled System Structure

2.1. Solar Collector

Solar energy, as a clean and renewable energy source, has drawn significant attention in recent years. SC is a device that can convert solar energy into heat energy. It is widely used in hot water supply [17–19], heating [20–22] and industrial heating [23–25]. The fundamental working principle of the SC is to transform light energy into heat energy by absorbing solar radiation and then transfer the energy through the heat–transfer medium. The entire process generally consists of three steps. The first step is solar–radiation absorption. The absorber plate of the collector (usually made of metal material and coated with a selective absorption coating) absorbs sunlight and converts it into heat energy. The second step is to transfer heat energy to the working medium inside the collector by means of heat conduction, convection, and radiation. The third step is thermal energy output, and the heated working medium transports the thermal energy to the heat storage system or the use end through the pipeline.

According to different structures, as shown in Figure 1, SC can be divided into three categories, flat plate collectors [26–28], vacuum tube collectors [29–31], and concentrating collectors [32–34]. Among them, the flat plate collector and the vacuum tube collector have certain similarities in working principle, and the working principle of the two collectors is quite different from that of the concentrating collector. Flat plate collectors and vacuum tube collectors mainly heat the internal heat transfer medium by absorbing solar radiation energy, while concentrating collectors use optical concentrating elements to concentrate solar rays onto smaller absorbers to achieve higher energy density collection.



Figure 1. Three types of SCs.

A flat plate collector is the most common type of SC, which is made up of a transparent glass cover, heat-absorbing plate, and thermal insulation layer. Its advantages are simple structure, low cost, and suitable for home and small- and medium-sized solar water heating systems. However, its heat collection efficiency is greatly affected by the ambient temperature, especially in winter and low light conditions.

The vacuum tube collector is composed of several vacuum glass tubes arranged in parallel. Each vacuum tube has an endothermic component, which can be a straight tube heat absorption tube, or a U-tube. U-tubes are usually made of metal materials (such as copper) with high thermal conductivity. The U-tube is symmetrically distributed in the vacuum tube. The bending part of the U-tube is usually located in the center of the

vacuum tube or near the center. The two ends are connected with the inlet and outlet pipes, respectively, to realize the circulating flow of the working substance in the tube and absorb the heat. The advantage of this arrangement is that the two branches of the U-tube can be relatively balanced when receiving solar radiation. This structure design is conducive to improving the heat transfer efficiency, so that the vacuum tube collector can more effectively convert solar energy into heat energy. Due to the superior vacuum insulation performance, vacuum tube collectors can effectively reduce heat loss, especially in cold climates. This type of collector is widely used in solar water heaters and heating systems in cold regions.

The concentrating collector uses a mirror or lens to concentrate sunlight onto the surface of a smaller receiver to produce a higher temperature. According to the different ways of focusing, it can be divided into two types, linear focusing and point focusing. Concentrating collectors are commonly used in solar thermal power generation systems and high-temperature industrial heating. Its advantage is that it can produce higher temperatures, but its structure is complex, the cost is high, and it requires an accurate solar tracking system to maintain high efficiency.

2.2. Air Source Heat Pump

The ASHP technology was first born in 1924, but it did not attract much attention at that time. It was not until the 1960s that it gradually came into people's vision and gained attention [35]. ASHP is a kind of high-efficiency and energy-saving equipment. As shown in Figure 2, it uses the heat in the air to transfer low-grade heat energy through components such as compressors, evaporators, and condensers and upgrades it to high-temperature heat energy for heating. Its basic working principle is based on the inverse Carnot cycle of the heat pump. The ASHP absorbs heat from the outside air, and even in the lower temperature environment, the air still contains a certain amount of heat energy. The refrigerant evaporates in the evaporator by absorbing the heat in the air through heat exchange with the air and becomes gaseous. The heated gaseous refrigerant enters the compressor, and the compressor compresses the refrigerant gas to greatly increase its temperature and pressure. The compressed high-temperature and high-pressure gas is the main heat source in the heating process of a heat pump. The high-temperature and high-pressure refrigerant gas enters the condenser. Through heat exchange with the water or air that requires heating, it transfers heat to the medium within the heating system, thus realizing heating. After the refrigerant releases heat in the condenser, it gradually cools and condenses into liquid. The liquid refrigerant reduces the pressure through the throttle valve, and the temperature also decreases and enters the next cycle. After throttling, the low-pressure refrigerant enters the evaporator again and continues to absorb heat from the outside air. Through this cycle, the ASHP can extract heat from the ambient air and use it for indoor heating. Although the ambient temperature is low, there is still enough heat in the air for use. It is an efficient and environmentally friendly heating technology, which is widely used in residential [36–38] and industrial fields [39–41]. ASHP has many advantages, but there are also some disadvantages. The performance of ASHP is greatly affected by the external air temperature. In the low-temperature environment (especially below -10 °C), the heat in the air is reduced, and the heating efficiency of the ASHP is significantly reduced. It may even need to rely on electric auxiliary heat to maintain heating, which will lead to increased energy consumption. Compared with the traditional heating modes, the cost of initial equipment purchase, installation, and supporting transformation of the ASHP system is higher. Although the long-term operation is energy-saving, the initial investment is a large expenditure for some users. In cold and humid climates, ASHP outdoor units may frost over, affecting the heat transfer efficiency.

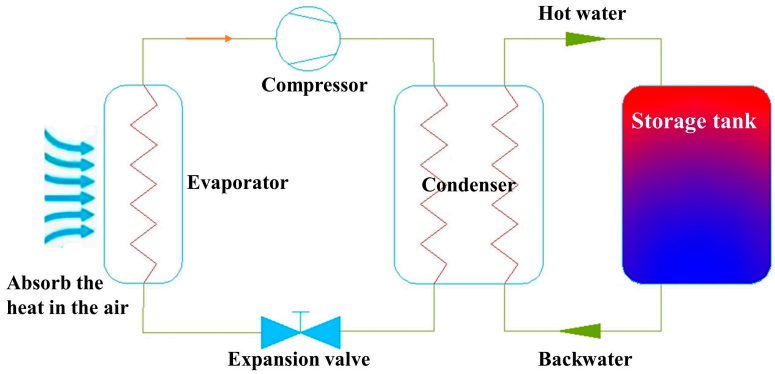

Figure 2. Schematic of the ASHP system.

2.3. S–ASHP System

Jodan et al. [42,43] proposed in the middle of the last century that solar-coupled heat pumps can not only improve the efficiency of solar energy collection but also improve the performance of heat pump systems. The S–ASHP system consists of two parts, solar energy and ASHP. The system is characterized by the organic integration of SC technology and ASHP technology, giving full play to the advantages of the two. This coupled system can be divided into two categories, DX–S-ASHP and IDX–S-ASHP. The DX–S-ASHP is relatively simple, and the evaporator of the ASHP is usually directly combined with the SC. Solar radiation increases the temperature of the collector, and the air directly absorbs the heat on the surface of the SC in the evaporator to complete the evaporation process. In this way, the solar energy can be directly used by the heat pump, which reduces the intermediate heat-transfer link and improves the energy utilization efficiency. However, at the same time, the design and material requirements of the evaporator are also higher, and the evaporator needs to be able to adapt to the high temperature and complex environment of the SC. The IDX–S-ASHP is more complex and can be subdivided into three main configurations—series, parallel, and hybrid—according to different requirements and scenarios. In a series solar–air source heat pump coupled system (Series IDX–S-ASHP), the SC and the ASHP are connected successively in the heating circuit. The SC first heats the fluid, and if the heat generated can meet the demand, the heated fluid is directly used for heating or supplying domestic hot water. However, when the solar heat is insufficient, the fluid initially heated by the SC enters the ASHP, where it receives secondary heating until the desired temperature is reached. This system can make full use of solar energy and reduce the operating time of the ASHP, but it needs a precise control strategy to coordinate the working sequence and flow of the two; otherwise, it is prone to energy waste or unstable heating. In the parallel solar–air source heat pump coupled system (Parallel IDX–S-ASHP), the SC and the ASHP have their own independent circulation loops, which can work simultaneously or independently according to the actual situation. When the solar energy is sufficient, the SC alone provides heat for the hot water or heating system. When solar energy is insufficient, the ASHP operates independently. When the demand for hot water is large or solar heating cannot meet all the needs, the two can work at the same time. The system has high flexibility and relatively simple control but requires more installation space and more accurate equipment capacity matching. The hybrid solar–air source heat pump coupled system (Hybrid IDX–S-ASHP) is a combination of series and parallel characteristics. Under different working conditions, through complex control strategies, it can flexibly switch series or parallel working modes, or operate in a special hybrid mode at the same time. It can achieve more optimized collaborative work of solar energy and ASHP according to complex and changeable environmental conditions and user needs, but the complexity of its control and design is also correspondingly higher. These different forms of coupling systems provide a variety of solutions to meet different energy needs and environmental conditions.

3. DX–S-ASHP System

The DX–S-ASHP adopts an integrated combination of an SC and an ASHP evaporator, allowing the working fluid to complete the evaporation process in the SC. As shown in Figure 3, the system mainly consists of components such as evaporator/SC, compressor, condenser, expansion valve, heat storage water tank, etc. The refrigerant enters the evaporator/SC through an expansion valve, absorbs solar radiation/air energy, and evaporates into refrigerant steam. The compressor then compresses it into high-temperature and high-pressure refrigerant steam, which enters the condenser and is condensed into refrigerant liquid while providing hot water to the user. Finally, the refrigerant liquid enters the evaporator/SC again through the expansion valve for heat absorption and evaporation, completing a cycle. The remarkable feature of the system is that it can effectively reduce the operating problems caused by the frosting of outdoor units, and the performance of the system increases with the increase in solar radiation. On sunny days, the average solar radiation is 610 W/m^2, and the heating time of the system water tank will be significantly shortened. Solar radiation is greatly affected by cloudy days, and the average solar radiation is 158 W/m^2, but the system can still meet the heating demand to a certain extent [44].

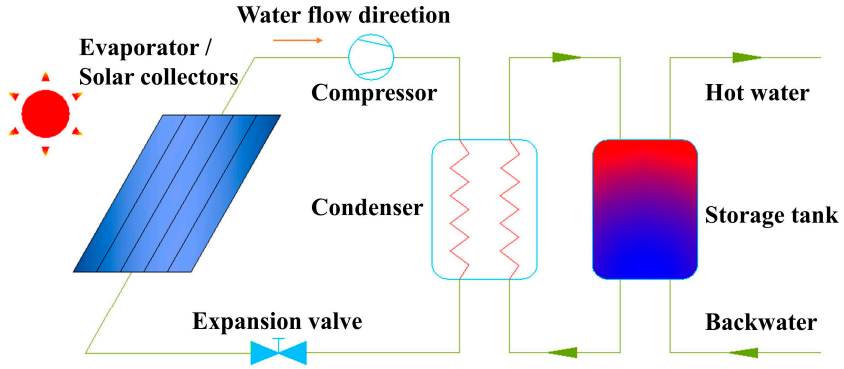

Figure 3. Schematic of the DX–S-ASHP system.

In the study of DX–S-ASHP, the evaporator is the key component of the heat pump, and the optimization of its structural design is particularly important, from Table 1. Traditional simple shell-type evaporators have some limitations in heat exchange efficiency and energy efficiency. In order to overcome these shortcomings, researchers continue to explore more efficient evaporator design, in order to improve the heat exchange effect while reducing energy consumption. Dong et al. [45] built a direct expansion solar air source heat pump experimental system, using R407c as the refrigerant. By comparing the heating performance of the ordinary evaporator heat pump system and the solar finned tube evaporator heat pump system, it is proved that the system with solar finned tube evaporator has better heating performance and low partial load rate. Ran et al. [46] put forward a new type of hybrid solar–air source heat pump, which is characterized by the use of a multi-functional evaporator with thermosyphon. Two different working modes of thermosyphon or heat pump are selected by different solar irradiance. When the solar irradiance is greater than 300 W/m^2, the system is provided by the solar thermosyphon mode. Hot water does not consume compressor power. In contrast to the SC heating alone system, the energy saving rate can reach 56–66%, and the energy saving rate can reach 20–48% in contrast to the ASHP system. Ma et al. [47] designed a new type of solar/air direct expansion heat pump system, which combines SC and ASHP evaporators. The heating capacity of the system is about 70% higher than that of the ASHP, and the COP value can still reach 3.46 at low temperatures of 0–8 °C. Chinnasamy et al. [48] put forward a dual–source evaporator for SAHP–DX, as shown in Figure 4. On sunny days, the COP value of the solar air source mode SAHP–DX–SAM system varies from 5.1 to 2.6. When the solar irradiance is low or no radiation, the COP value of the air source mode SAHP–DX–AM system is 4.1–2.2, and the average COP of SAHP–DX–SAM is greater than that of SAHP–DX–AM.

Table 1. Optimization of evaporator and collector of DX–S-ASHP system.

References	Type	Refrigerant	Optimize the Technical Route	Result
[45]	Experimental test	R407c	A solar finned tube evaporator is proposed.	In relation to the same type of conventional ASHP, it has better heating performance.
[46]	Simulation	R410a	A multifunctional evaporator with thermosyphon is proposed.	In relation to the ASHP system, the energy-saving rate can reach 20–48%.
[47]	Experimental test	–	The SC and heat pump evaporator are combined.	In relation to the ASHP, the heating capacity is increased by about 70%.
[48]	Experimental test	R410a	A dual-source plate evaporator.	Significantly improve the system performance
[49,50]	Simulation	–	A new type of triangular solar air collector-assisted air source heat pump is proposed.	The COP value under the best working mode is increased by 64.4%.
[51]	Experimental test	R134a	Apply the concentrator to the system.	The heating capacity has gone up by 5.9% and the total efficiency has been elevated by 9.5%.

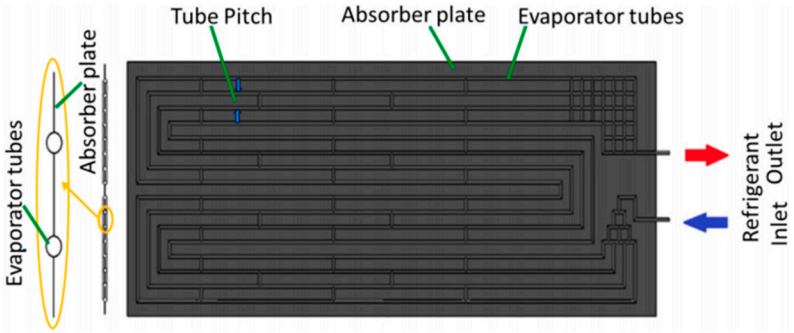

Figure 4. Schematic of dual-source evaporator [48].

From Table 1, the optimization of the collector can improve the overall performance of the system. As the front-end device of energy conversion, the efficiency of the collector directly affects the heat energy acquisition and transformation efficiency of the whole system. Although conventional flat plate collectors and vacuum tube collectors can meet the needs of energy harvesting to a certain extent, with the development of technology, the demand for improving its performance and efficiency is increasing. Therefore, many scholars continue to explore innovative collector designs to achieve higher energy efficiency and better adaptability. The progress of collector technology is mainly focused on improving the efficiency of heat collection and enhancing the adaptability of the system. Yan et al. [49,50] used a system that operates by coupling a triangular solar air collector and an ASHP. The system can adjust its operating mode according to the external environmental parameters, and the distributed boundary equation of the optimal operating mode is corrected by establishing a mathematical model. After correction, the COP value of the system in the best working mode is increased by 64.4%. Song et al. [51] proposed an efficient and multi-functional concentrating solar–air centralized heat pump system (MC–SA–HP), which can simultaneously provide power generation, heating, and cooling through different operating strategies. In relation to the flat panel photovoltaic system, the power generation of the system has risen by 71.8%. The heating capacity has increased by 5.9%. The overall power generation has gone up by 12.6%, the total efficiency has grown by 9.5%, and the COP_{PVT} has increased by 7.3%.

External environmental factors have an important impact on the operation effect and efficiency of the system. From Table 2, different environmental conditions, such as ambient temperature and solar irradiance, will significantly affect the overall performance and

efficiency of the heat pump system. For the design and optimization of these systems, it is crucial to understand the mechanism of external environmental factors. By analyzing the influence of environmental factors on the system, it can help to optimize the operating parameters and design of the system, so as to improve the overall efficiency of the system. Fernández-Seara et al. [52] experimentally evaluated the efficacy of a direct expansion solar-assisted heat pump water heating (DX–SAHPWH) system under conditions of zero solar radiation, as shown in Figure 5. An artificial climate chamber was established to simulate zero solar radiation conditions. The SC was placed in the climate chamber, and the air temperature and humidity were adjusted through the internal climate control system. In this way, working conditions with zero solar irradiance and a stable ambient air temperature were set up. The characteristic COP of the DX–SAHPWH system evaluated under the condition of zero solar irradiance is 3.23. Song et al. [53] designed and studied three hybrid heat pump systems based on different concentrators. A factor analysis was performed by setting different concentration ratios, water temperature, ambient temperature, and solar irradiance. In the FPV–SAHP system, the effects of ambient temperature, water temperature, and solar irradiance on the system under two concentration ratios were designed and discussed. The overall efficiency of the system grew as the ambient temperature rose, while the increase in water temperature had a minimal impact on the system's total efficiency. Cao et al. [54] studied the effects of solar radiation, ambient air temperature, SC area, condenser tube length, collector tube outer diameter, fin thickness, collector thermal conductivity, and other design parameters on the performance of DX–SAHPWH, as shown in Figure 6. It provides ideas for the optimal design of each component of the system. Dai et al. [55] calculated the operating performance of the direct expansion solar air source heat pump under all operating conditions and used EXCEL language to write the program. The simulation outcomes suggest that the collector surface temperature and heat collection efficiency are affected by solar irradiance and ambient temperature, and there is a critical heat loss temperature. The highest heating performance coefficient of the composite system in summer is 7, and the lowest heating performance coefficient in winter is 3.23.

At the same time, Fang et al. [56] mathematically modeled the collector, compressor, condensate tank, expansion valve, etc., of the direct expansion system, and further analyzed the operating characteristics of the system throughout the year by using the model and system simulation program. When the running time of the heat pump system keeps increasing, the evaporation temperature tends to rise gradually, and the difference between it and the ambient temperature reduces gradually. Under such circumstances, the proportion of heat absorbed by the collector/evaporator from the air keeps decreasing, which consequently results in a gradual reduction in the instantaneous COP value of the system. Cai et al. [57] established a new type of air source hybrid solar-assisted heat pump (AS–SAHP). A mathematical model was established to analyze the effects of ambient temperature, solar irradiation, and evaporation area on evaporation. The results indicate that the average COP of the AS–SAHP system is 2.71 under 100 W/m^2 solar irradiation and 10 °C ambient temperature. In comparison with the ASHP and the DX–SAHP systems, the AS–SAHP system shows superior performance. Yu et al. [58] proposed a vacuum tube direct expansion solar heat pump system. Experimentally, the effects of solar irradiance and circulating water temperature on the system performance under typical working conditions were investigated, and the dynamic performance of the system under the condition of compressor frequency conversion was explored.

Table 2. Study on the influence of the external environment on the DX–S-ASHP system.

References	Type	Refrigerant	Optimize the Technical Route	Result
[52]	Simulation	R134a	In different environments, through the theoretical analysis of the components.	The COP of the system is 3.23 under the condition of zero solar radiation.
[53]	Simulation	–	Different concentration ratios, water temperature, ambient temperature, and solar irradiance were set for factor analysis.	The total efficiency increases with the increase in ambient temperature.
[54]	Simulation	R134a	The effect of system design parameters on performance is investigated.	It provides ideas for the optimal design of each component of the system.
[55]	Simulation	R134a	The variation in heating performance with ambient temperature and solar irradiance was studied.	The highest heating performance coefficient of the system is 7 in summer and the lowest is 3.23 in winter.
[56]	Simulation	R–134a	Mathematical modeling and analysis of the system.	The greater the solar irradiance and the higher the ambient temperature, the shorter the heating time of the system.
[57]	Simulation	–	The effects of ambient temperature, solar irradiation, and evaporation area on evaporation were analyzed.	The average COP of the system is 2.71 under 100 W/m^2 solar irradiation and 10 °C ambient temperature.
[58]	Experimental test	R134a	The effects of solar irradiance and circulating water temperature on the performance of the proposed system are analyzed.	Increasing the solar irradiance and reducing the circulating water temperature are beneficial to improve the system's performance.

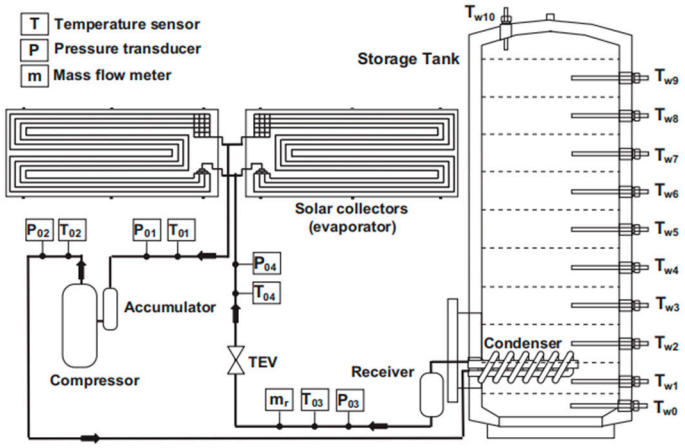

Figure 5. Schematic diagram of the DX–SAHPWH system [52].

From Table 3, the distribution of refrigerant plays an important role in the optimization of system performance. The refrigerant is responsible for transferring heat between the evaporator and the condenser. Effective refrigerant distribution can not only improve the overall efficiency of the heat pump but also optimize the system performance under different operating modes. Li et al. [59] proposed a solar/air hybrid dual-source assisted heat pump (S–A–AHP) water heater, as shown in Figure 7. On this basis, a quasi-steady-state mathematical model is established, and the mode-switching standards and operational performance are researched. The simulation outcomes indicate that the mass flow ratio of the cooling medium (that is, the ratio of the photovoltaic/collector/evaporator to the entire system) is more appropriate compared to the direct utilization of environmental factors, and the critical ratio for the switching between the solar air mode and the solar mode is approximately 0.75. Liu et al. [60] put forward a new type of solar/air dual-source heat pump system, and it is studied by controlling the refrigerant flow. The results indicate that the system performance is enhanced by optimizing the refrigerant flow ratio in the

SC and evaporator. When the ratio of the refrigerant flowing into the SC is 0.6 to 0.7, the cooling effect is optimal. Cai et al. [61] proposed a parallel evaporator dual-source heat pump, developed two different evaporation side refrigerant distribution control schemes, and optimized the performance of the solar–air composite source multi-functional heat pump in the space heating mode and the water heating mode by adjusting the distribution of the refrigerant on the evaporation side.

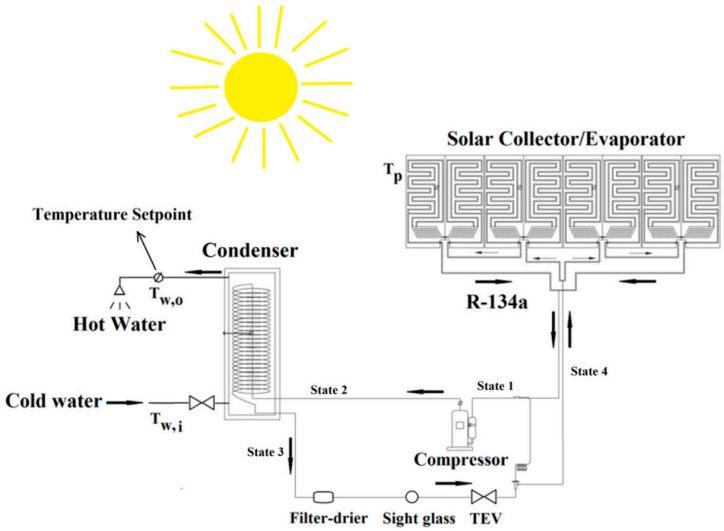

Figure 6. Schematic diagram of the DX–SAHPWH [54].

Table 3. Study on the influence of refrigerant on the DX–S-ASHP system.

References	Type	Refrigerant	Optimize the Technical Route	Result
[59]	Simulation	R134a	The mass flow ratio of the refrigeration medium.	The critical ratio of switching between solar air mode and solar mode is about 0.75.
[60]	Simulation	R22	Optimize the flow ratio of refrigerant in SC and evaporator.	When the ratio is 0.6–0.7, the cooling effect is the best.
[61]	Simulation	–	Regulate the distribution of refrigerant on the evaporation side.	The performance of the system in space heating mode and water heating mode is optimized.
[62]	Simulation	R290, R22, R410A	The system performance coefficient, heat collection efficiency, and heating power of R290, R22, and R410 A are compared and analyzed.	The COP value of the R290 system is higher than the other two.
[63]	Simulation	R134a, R290, R410A, R717	The performance of the system under four different working fluids R134 a, R290, R410 A, and R717 was compared.	As a cooling medium, R717 has higher system energy efficiency than other working fluids.

It is very important to select the appropriate working medium (refrigerant). From Table 3, different working fluids have different thermodynamic properties, such as boiling point, critical temperature, and pressure, which directly affect the energy efficiency and operation effect of the system. Kong et al. [62] compared the direct expansion solar heat pump system using R290, R22, and R410A under the same external environmental parameters, and found that the COP value of the R290 system is higher than that of the other two, and the COP value of the system can be improved by changing the external environmental parameters. The influence of different working fluids on direct expansion. Yang et al. [63] proposed a heating system combining solar photovoltaic thermal energy collector (PVT) and ASHP, as shown in Figure 8. By switching the working mode, the

power generation efficiency of photovoltaic panels can be improved while effectively utilizing solar thermal energy. Simultaneously, R134a, R290, R410A, and R717 were chosen as candidate working fluids for removing the heat from the back of the photovoltaic panel. When R717 is utilized as the cooling medium at the back of the photovoltaic panel, both the energy utilization coefficient and energy efficiency of the system are superior to those of other working substances.

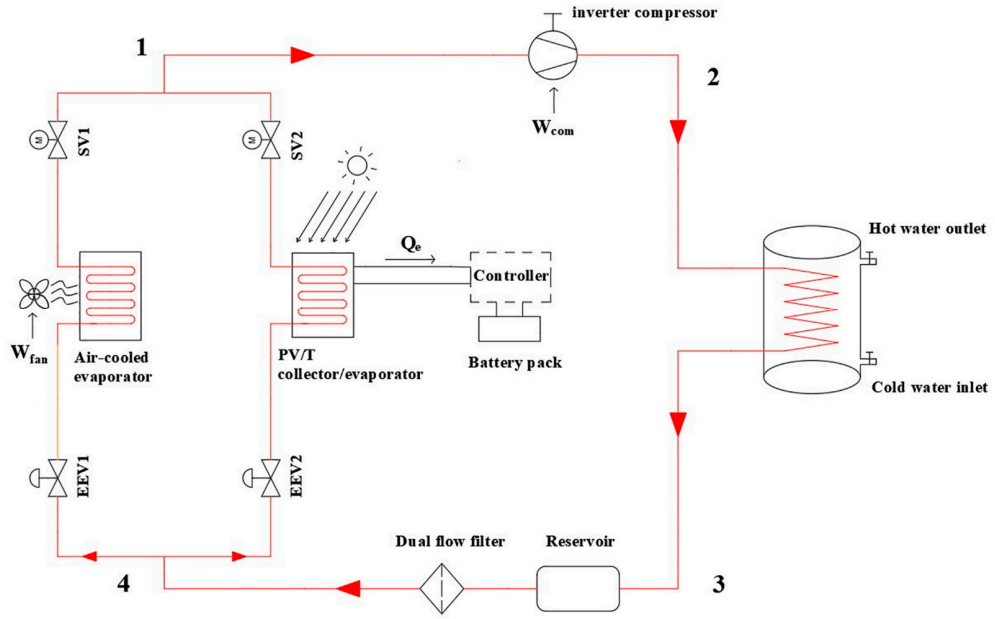

Figure 7. Schematic diagram of the solar/air dual source assisted heat pump water heater [59].

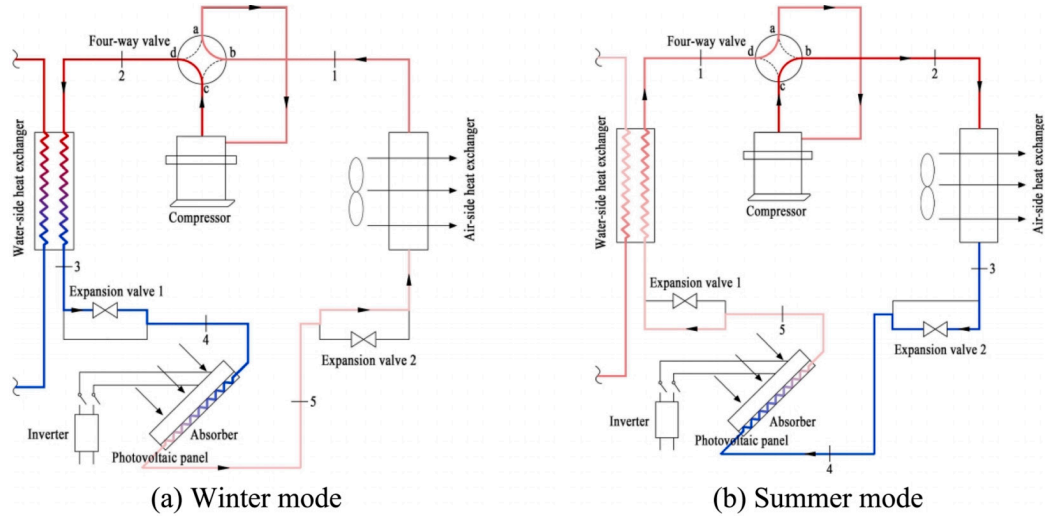

Figure 8. Schematic diagram of the solar PVT collector coupled with switchable ASHP system [63].

4. IDX–S-ASHP System

In the design of the IDX–S-ASHP system, the SC and the evaporator of the ASHP unit are separated. In this system, when the heat-collecting medium absorbs solar energy, it is heated in the SC. Subsequently, the heat is transferred to the evaporator, and through this evaporator, the heat is then transferred to the heat pump unit, thereby achieving the goal of providing heat. Due to their high energy utilization efficiency and low-carbon emissions in environmental protection, IDX–S-ASHP systems have been widely utilized [64].

4.1. Series IDX–S-ASHP System

The Series IDX–S-ASHP system mainly consists of SC, heat storage tanks, evaporators, compressors, condensers, expansion valves, and other components. As shown in Figure 9, the SC and the ASHP are connected in series in the heating circuit in order. The evaporator of the ASHP is connected to the heat storage tank, which can absorb the heat stored in the heat storage tank. In addition, the water tank is also connected to the condenser of the ASHP to provide heat to the user. When the solar irradiance is greater than 100 W/m^2, the heat storage tank can sustainably maintain a higher water temperature inside and provide the heat required by the evaporation section of the heat pump. At this time, the heat storage tank can sustainably store solar heat energy. When the solar irradiance is less than 100 W/m^2, the hot water stored in the heat storage tank can continue to provide heat for the evaporation section of the heat pump, which to some extent alleviates the fluctuation of heating in the Series DX–S-ASHP system when solar irradiance is unstable [65–67]. However, as the solar irradiance energy of the system continues to decrease, the water temperature in the heat storage tank will also continue to decrease, and the working performance of the heat pump will also decrease.

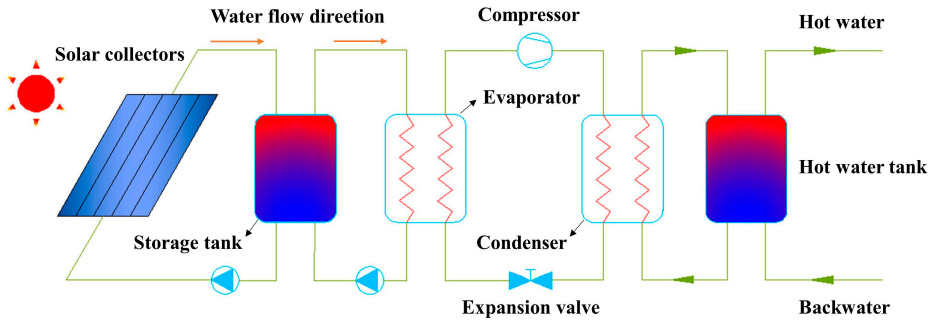

Figure 9. Schematic of the Series IDX–S-ASHP system.

The choice of refrigerant plays a crucial role in the design and optimization of the system. Although traditional refrigerants, such as freon, have been widely used in history, their negative effects on the environment have been widely recognized, especially the destruction of the ozone layer and the potential for global warming. Therefore, in recent years, more and more new refrigerants have been introduced to improve the overall efficiency and sustainability of the system. New refrigerants, such as R32 [68–70], R290 [71–73], R744 [74–76], R1234yf [77–79], and R407C [80–82], not only have low global warming potential (GWP) and ozone depletion potential (ODP) but also can maintain excellent thermodynamic performance under a wider range of operating conditions, thus playing a greater role in the heat pump system. It is very important to select appropriate refrigerants to improve the performance of the system. Bellos et al. [83] studied a solar heating power generation production system suitable for building applications. The combined heat and power system consists of a hybrid photovoltaic (or PV/T) collector and a heat pump driven entirely by a SC. An innovative multi-objective program is adopted, with heating and power generation as the objective functions. The heat pumps with seven different working fluids were optimized under the steady-state conditions of the heat pump. Under the steady-state conditions of the optimal fluid R32, the energy utilization efficiency can reach 60.85%. Wang et al. [84] introduced a new type of indirect expansion solar-assisted multifunctional heat pump system (IX–SAMHP), which uses R407C as a refrigerant. The system comprises three heat exchangers along with one refrigerant receiver. Among them, the water-cooled heat exchanger is linked in parallel to the indoor and outdoor air-cooled heat exchangers. Tests indicate that in comparison with solar water heaters, IX–SAMHP is capable of generating heat with a lower power consumption on cloudy days.

In the design and operation of the system, low-temperature compensation is a key optimization strategy, from Table 4. The low-temperature environment generally results in a reduction in heating efficiency, because the low temperature of the external air will

affect the evaporation temperature of the refrigerant, thereby reducing the COP of the heat pump. In order to overcome this problem, researchers continue to explore various low–temperature compensation technologies to improve the operating efficiency of heat pumps in cold climates. The introduction of low-temperature compensation technology can remarkably enhance the stability and energy efficiency of the system in low-temperature conditions, thereby broadening the application range of the heat pump. Long et al. [85] proposed a dual heat source integrated heat pump evaporator with solar energy and air as heat sources, as shown in Figure 10. The refrigerant coil and water coil are installed and arranged in the evaporator in a certain way. The supply of hot water to the evaporator is capable of increasing the evaporation temperature of the refrigerant and the heat pump's COP. As the average water temperature of the evaporator grows from 14.6 °C to 39.5 °C, the COP of the heat pump experiences a 15% increase. Liu et al. [86] took the solar-assisted air source heat pump system as the research object and used the two–heat combined gas-liquid heat exchanger as the core component. Under various environmental parameters, in contrast to the single ASHP system, the composite heat pump system boasts higher energy efficiency and enhances energy utilization efficiency.

Table 4. Study on the influence of refrigerant and low-temperature compensation on the Series IDX–S-ASHP system.

References	Type	Refrigerant	Optimize the Technical Route	Result
[83]	Simulation	R404A, R32, R1234yf, R290, R600a, R245fa R152a	R404A, R32, R1234yf, R290, R600a, R245fa and R152a were optimized.	The optimal fluid is R32, and the energy utilization efficiency can reach 60.85%.
[84]	Simulation	R407C	The refrigerant receiver ensures smooth switching between different operating modes.	It has the advantages of energy–saving operation mode and good applicability to different weather conditions.
[85]	Experimental test	R22	An integrated solar–air source heat pump evaporator with solar and air heat sources is designed.	The COP of the system increases by 15%.
[86]	Experimental test	R22	A double heat combined gas-liquid heat exchanger was designed.	Improve the efficiency of energy utilization.

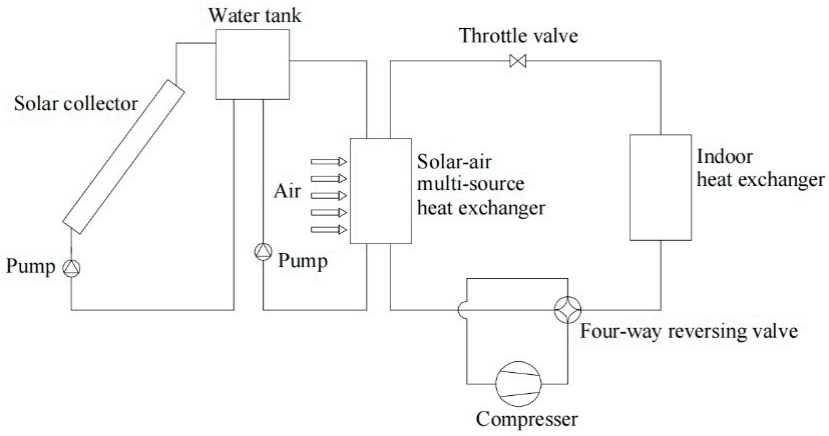

Figure 10. System diagram [86].

4.2. Parallel DX–S-ASHP System

The Parallel DX–S-ASHP system is mainly composed of components such as a SC, compressor, condenser, evaporator, expansion valve, and heat storage water tank, as shown in Figure 11. SC and ASHP are relatively independent and can operate separately or work together according to different weather conditions and heating requirements. Among them, ASHP uses air as a low-temperature heat source, drives the compressor through electric

energy, and the evaporator absorbs heat from the air and transfers it to the water in the hot water storage tank. Wang et al. [87] established a parallel coupled system. On sunny days, SC is preferentially used for heating. When SC alone cannot reach the set temperature of the hot water storage tank at 35 °C, ASHP is started, and the two heat sources heat the water tank at the same time. When the water tank reaches the set temperature, ASHP stops working, SC can run for 8 h, and the heat pump runs for 8 h. On cloudy days, the solar irradiance is insufficient, the SC only runs for 6.5 h, and the heat pump runs for 9.5 h. On rainy days, SC stops running and ASHP runs independently for 16 h to provide heat. This coupled operation mode is less affected by solar irradiance fluctuations, as solar energy and air sources do not affect each other and can operate independently. It not only effectively solves the intermittently occurring solar energy system in independent operation and frosting problems of ASHP, but also increases the heating capacity of the system, and reduces the energy consumption of ASHP by improving the efficiency of the system. In the heating mode, the Parallel DX–S-ASHP system heating efficiency is higher [88].

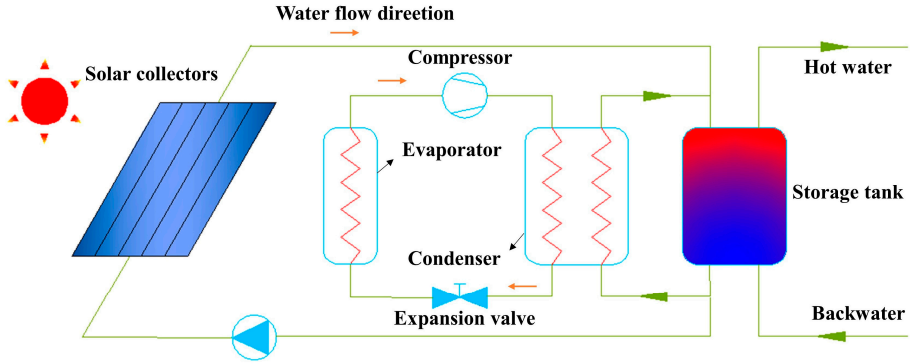

Figure 11. Schematic of the Parallel IDX–S-ASHP system.

Over the recent period, heat load forecasting has made remarkable progress based on advanced machine learning and data analysis techniques. Especially in renewable energy systems such as ASHPs and solar energy, load forecasting can help optimize the operating efficiency of the system, improve the efficiency of energy use, and reduce energy waste, as shown in Table 5. Hu et al. [89] studied the hourly load forecasting of variable frequency solar–air source heat pump systems based on Long Short-Term Memory (LSTM), and proposed a short-term load forecasting model of Variable Frequency Solar Air Source Heat Pump system (VFAP) based on LSTM neural network, which provided a basis for the matching of load and heat pump working conditions. Liu et al. [90] first gave the prediction method of the heating capacity of ASHP based on the dynamic equation of the ASHP heating system, and then gave the operation steps of the scheduling strategy from the perspective of energy. When the scheduling strategy was adopted on that day, the running time of the heat pump was reduced by 1 h compared with that of the default strategy, and the utilization rate of solar energy was significantly increased. Lu et al. [91] constructed a coupled thermal model of ASHP and SC. Using the K-Nearest Neighbors (KNN) supervised learning algorithm in machine learning, the hourly temperature and humidity of the environment, the water consumption in the previous period, and the number of weeks were used to realize the hourly prediction of the hot water load. The dynamic control strategy based on the water temperature baseline and the water level baseline method was used to dynamically control the water supply and heat pump.

Table 5. Research on load forecasting and key parameter optimization of Parallel IDX–S-ASHP system.

References	Type	Refrigerant	Optimize the Technical Route	Result
[89]	Simulation	–	System short-term load forecasting based on LSTM neural network.	Reduce the use of ASHP, thereby reducing energy consumption purposes
[90]	Simulation	–	The heating capacity of ASHP is predicted to realize the control of heat pump.	Shorten the running time of the heat pump.
[91]	Simulation	R22	The KNN algorithm is used to realize the hourly prediction of hot water load.	The energy consumption of the system is reduced by 7.55–20.36% compared with the original control scheme.
[92]	Simulation	–	The Hooke–Jeeves algorithm is used to optimize the key parameters of the system.	The annual energy consumption is reduced by about 3.9%.
[93]	Simulation	–	The Hooke–Jeeves algorithm is used to optimize the key parameters of the system.	After optimization, the unit heating cost is saved by about 20.6%.
[94]	Simulation	R410A	A method for calculating the economic optimal f and collector area of the system is proposed.	Maximize solar energy potential and reduce system cost.
[95]	Simulation	–	Combined with the iterative optimization of GenOpt program, the optimal installation angle and size are obtained.	The coefficient of thermal performance of the system is 4.6.
[96]	Simulation	R410a	Optimization of system performance and key parameters.	The optimal values of SC area, collector angle, and tank volume are 225 m^2, 45°, and 30 m^3, respectively.
[97]	Simulation	–	The effects of ambient temperature, effective collector area, and cumulative heat capacity of the collector on system performance are studied.	The dynamic change in ambient temperature and instantaneous solar irradiance is the main reason for the error in heat balance.

The reasonable adjustment of key parameters is crucial to the improvement of system performance. Optimizing these parameters can significantly improve the energy efficiency of the system. Ma et al. [92] studied the optimization of a solar-assisted air source heat pump hot water system and optimized the key parameters of the system by the Hooke–Jeeves algorithm. The optimized variables include tank volume, collector area, inclination angle, azimuth angle, and heat pump power, aiming to improve the energy efficiency of the system. Zhang et al. [93] adopted the Hook–Jeeves algorithm to optimize the area of the collector, the angle of the collector, the volume of the water tank, the heating capacity of the heat pump, and the start–stop temperature difference in the heat pump. After optimization, the unit heating cost was saved by about 20.6%. Zheng et al. [94] used TRNSYS 18 software to establish a solar-assisted air source heat pump (SAASHP) system to meet the needs of 480 students for bathing in hot water, focusing on the economic optimization of the design value of solar fraction (f) in the SAASHP water and hot water system. A method for calculating the economic optimal f and collector area of the SAASHP system is proposed to maximize the solar energy potential, reduce the system cost, and promote the application of solar water heating technology.

Wu et al. [95] used TRNSYS software to simulate the solar–air source heat pump composite heating system with an auxiliary heating device and analyzed the influence of the installation angle and area of the SC on the performance of the system. By combining the iterative optimization of the GenOpt program, the optimal installation angle and size are obtained. The results show that the average collector efficiency, solar fraction, and coefficient of performance (COP_{sys}) of the system increase first and then decrease with

the increase in collector inclination angle, and reach the maximum at 55°. Long et al. [96] studied the performance and optimization of key parameters of a solar air source heat pump (SASHP) heating system for office building heating under climatic conditions in Tibet and used TRNSYS to model and simulate the system. The findings indicate that for the climatic and environmental conditions in Tibet, the area of the SC and the volume of the water tank are the primary factors in the design of the SASHP system. Xu et al. [97] established the transient heat balance model of the system under sunshine time and non–sunshine time, as shown in Figure 12. The relationship between ambient temperature, effective heat collection area, and heating capacity was obtained. After calculation, it was discovered that the dynamic variations in ambient temperature and instantaneous solar irradiance were the principal reasons for the heat balance error. After several experimental measurements, it is difficult for ETC to convert solar irradiance energy into effective heat energy when the solar irradiance is lower than 300 W/m^2. (The effective input of divisible solar energy is often determined.) The heat loss is calculated within the effective time of non–solar energy.

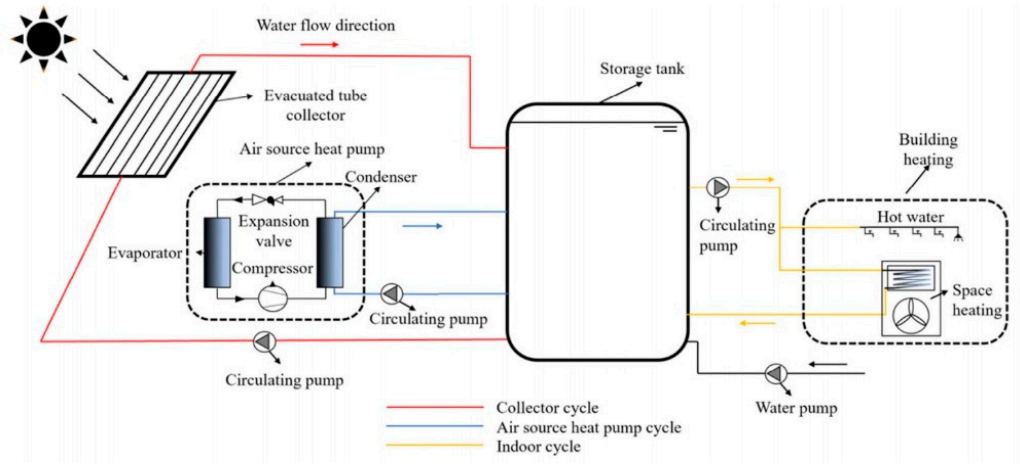

Figure 12. Schematic diagram of the system [97].

At the same time, in order to maximize the potential of solar energy, solar energy utilization can be improved by optimizing system design, improving system efficiency, and reducing operating costs, as shown in Table 6. Liu et al. [98] took the minimum life cycle cost of the system as the optimization goal, and established a joint optimization model of capacity configuration and heating network diameter of solar central heating system based on the Matlab platform. The genetic algorithm was used to solve the model, and the collaborative optimization model was used to design the solar central heating system, which could effectively match the solar guarantee rate with the water supply temperature and improve the utilization rate of solar energy. Wang et al. [99] analyzed the operation performance of the hybrid system and the mutual influence of hot water supply and space heating on the heat pump heating, solar water heating, space heating load and hot water heat loss. Liu et al. [100] established a solar fresh air (SFA) heating system model, and further established a solar–air source heat pump (SASHP) heating system. The average COP value of the SASHP system in the heating season is 6.22. The COP value of the SASHP system is 109.43% higher than that of the ASHP system, and the energy consumption and annual cost are 55.38% and 9.7% lower than those of the ASHP system, respectively.

Table 6. Optimization of evaporator and collector of Parallel IDX–S-ASHP system.

References	Type	Refrigerant	Optimize the Technical Route	Result
[98]	Simulation	–	The collaborative optimization model is used to design the solar central heating system.	Effectively avoid the solar energy guarantee rate of the design system is small.
[99]	Simulation	–	The interaction between hot water supply performance and space heating performance is analyzed.	The hot water flow rate has a significant effect on the instantaneous heat generation of the hybrid heating system.
[100]	Simulation	–	A SFA system was set up.	The system can reduce energy consumption by 55.38%.
[101]	Experimental test	–	The air source evaporator obtains heat from the outdoor air in the atmosphere by means of the air source side loop of a heat pump equipped with a solar–air source device.	Significantly improve the system COP and reduce energy consumption.
[102]	Experimental test	R134a	The water source evaporator is added to the existing solar-assisted ASHP drying system.	The system energy consumption is reduced by 17.15%.
[103]	Simulation	–	The operation characteristics and energy saving of the system with different optimization strategies are analyzed.	Reducing the start–stop temperature of the auxiliary heat source ASHP can effectively reduce the power consumption of the system.

By improving the structure of the evaporator, the heat exchange efficiency can be improved, the heat loss can be reduced, and the performance of the system can be improved. Li et al. [101] proposed a solar–air source coupled system, which extracts heat from the outside air through an air-source evaporator and introduces it into the air-source side circuit of a heat pump with a solar–air source device. The results show that the total energy efficiency of the system reaches 2.22, 2.22, 2.3, and 2.62, respectively, for 4 consecutive days. At the same time, the efficiency of SC has also increased to more than 33%, with good results. Hou et al. [102] put forward a solar-assisted multi-heat source heat pump (SMSHP) drying system. In this system, a water source evaporator was added to the existing solar-assisted air source heat pump drying system. The results indicate that compared with the ASHP drying system, the energy consumption of the SMSHP drying system is decreased by 17.15%, while the coefficient of performance is increased by 7.3%. At the same time, the start–stop control strategy of ASHP is also an important part of improving system performance. Yu et al. [103] established a simulation model of an air source heat pump-assisted solar water heating system through TRNSYS. The temperature difference controller was used to control the start and stop of the ASHP, reduce the start and stop temperature of the ASHP, and decrease the operational energy consumption of the system.

4.3. Hybrid IDX–S-ASHP System

The Hybrid IDX–S-ASHP system is developed on the basis of the Series IDX–S-ASHP system, forming a more efficient and energy-saving heat pump heating scheme. The system is mainly composed of SC, heat storage water tank, compressor, condenser, evaporator, expansion valve, and other components, as shown in Figure 13. This coupled operation mode integrates the advantages of series and parallel, can improve the utilization efficiency of solar energy and air source at the same time, has good heating performance and energy conservation and environmental protection, and is widely used in space heating and domestic hot water. However, the Hybrid IDX–S-ASHP system has many components, a complex structure, and a high initial investment.

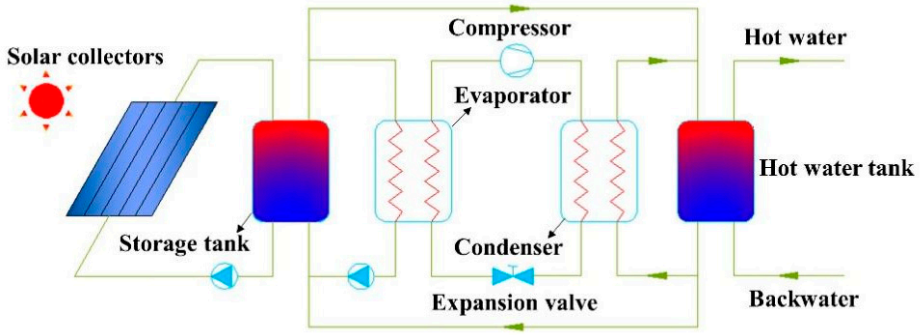

Figure 13. Schematic of the Hybrid IDX–S-ASHP system.

With the ceaseless development of renewable energy technology and the increase in global energy demand, the Hybrid IDX–S-ASHP system has received extensive attention due to its high efficiency and energy-saving characteristics. Huan et al. [104] proposed a solar-assisted heat pump system (SAHP) that can work in serial or parallel mode. The annual average COP value is 5.7, and the series–parallel system is 3.3 and 4.3, respectively. Compared with the series–parallel system, the combined system has a significant energy-saving effect. Yang et al. [105] used TRNSYS to model and simulate three solar–assisted air source heat pump systems in London, including series, parallel, and dual–source indirect expansion heat pumps. The simulation results show that the COP of the series heat pump is up to 5.5, but the requirements for SC and hot water storage tanks are large. In contrast, the COP of the dual-source heat pump and the parallel heat pump is slightly lower, 4.4 and 4.5, respectively, but the requirements for SC and hot water storage tanks are smaller. Yang et al. [106] set the hot water supply temperature of 40 °C, 45 °C, 50 °C, and 55 °C when modeling and simulating the heating system for one year under the weather conditions of London, Orton, and Aberdeen in the UK. The research discovered that, as the temperature of the hot water supply dropped from 55 °C to 40 °C, the annual seasonal performance coefficient (SPF) of London, Orton, and Aberdeen increased by 16.7%, 19.1%, and 15.4%, respectively. The results indicate that low-temperature heating can remarkably decrease the power consumption of the system.

The operation mode of the temperature control system of the hot water storage tank can automatically adjust the working state of the system, according to the temperature change in the hot water storage tank, so as to ensure the intelligent switching of the heating system between different heat sources and optimize the energy efficiency, as shown in Table 7. Gong et al. [107] proposed a heat pump system with two heat sources of solar energy and air source by switching composite heating. Based on the establishment of a thermodynamic mathematical model, a program was written to calculate the cycle characteristics and analyze the energy consumption of the new system. Based on experience, the start–stop control conditions for the solar flat plate collector and the solar–air source heat pump dual heat source heat pump unit were established, according to the temperature of the heat storage tank and the temperature difference between the inlet and outlet of the collector. In addition, the accuracy of the TRNSYS model was verified. Wang et al. [108] proposed a solar-assisted dual-source dual-compression coupled heat pump system. The three modes of system operation were determined by the temperature difference between the inlet and outlet of the SC system, and the energy consumption analysis was carried out under the three modes. Compared with the traditional ASHP, the whole heating period saves 8.72%. Li et al. [109] established a solar vacuum tube water heater–air source heat pump system (SETWH–ASHP). The system has three modes, solar water heater heating, ASHP heating, and solar vacuum tube water heater–air source heat pump system heating. The temperature of the hot water storage tank controls the three modes, and the system undergoes testing and simulation.

Table 7. Hybrid IDX–S-ASHP system research.

References	Type	Refrigerant	Optimize the Technical Route	Result
[107]	Experimental test	–	The influence of system design parameters on the energy consumption of the system is studied.	The system can reduce emissions by 22%.
[108]	Simulation	R134a	A dual source (air source and water source evaporator) dual compressor parallel process coupled heat pump is proposed.	Compared with the traditional ASHP, the whole heating period can save energy by 8.72%.
[109]	Experimental test	–	A solar vacuum tube water heater–ASHP system was established.	The maximum COP of the system is 3.6, the average COP is about 2.9, and the primary energy-saving rate is 66.4%.
[110]	Simulation	–	A compound parabolic concentrator–capillary SC is proposed.	The collector efficiency of the collector is high, which reduces the size of the collector and significantly reduces the cost.
[111]	Experimental test	R22	The unique combination of large flat plate SC and double source heat pump is adopted.	The percentage of solar energy in the whole heating season amounts to 31.8%, and the energy efficiency ratio of the system is 3.08.

As the core component of the SC system, the performance of the SC has a direct impact on the efficiency and economy of the whole system. Optimizing the design and operation parameters of collectors is one of the key means to improve the efficiency of solar heat utilization. The type, material selection, structural design, and installation angle of the collector will affect its heat collection efficiency and cost. In recent years, more and more research has focused on the development of efficient and low-cost collectors to improve the overall performance of the system. Yang et al. [110] proposed the numerical simulation of the composite parabolic concentrator–capillary solar collector (CPC–CSC) of the British solar-assisted ASHP heating system. The collector of CPC–CSC has high efficiency, small size, and significantly reduced cost. CPC–CSC is used as an SC to optimize the operation performance of the solar-assisted air source heat pump (SAASHP), as shown in Figure 14. The system is simulated by TRNSYS, and the influence of the SC area on system performance is analyzed, especially the influence of the collector area on system efficiency. Li et al. [111] established a large flat plate solar collector–air source heat pump (LFPSC–ASHP) combined heating system as shown in Figure 15. During the heating season, solar energy heating time takes up one-third of the total heating time. By optimizing the system configuration, particularly expanding the storage tank's capacity, the solar heating time can be prolonged, the system's energy consumption can be cut down, and the system's economic performance can be enhanced.

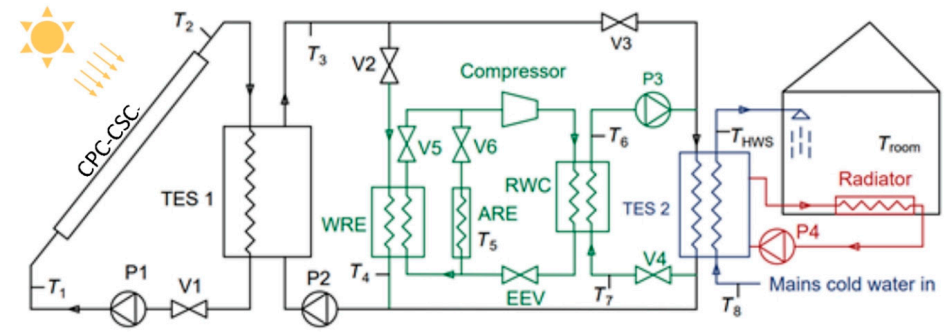

Seven loops in the heating system:
(1) Solar collector loop: SC-TES1-V1-PA-SC
(2) TES1-WRE loop: TES1-V2-WRE-P2-TES1
(3) ASHP loop: ARE-V6-Compressor-RWC-EEV-ARE
(4) space heating loop: TES2-Radiator-P4-TES2
(5) TES1–TES2 loop: TES1-V3-TES2-P2-TES1
(6) RWC-TES2 loop: RWC-P3-TES2-V4-RWC
(7) SWHP loop: WRE-V5-Compressor-RWC-EEV-WRE

SC: Solar collector
TES 1, TES 2: TES tank
V1 - V6: Valve
P1 - P4: Water pump
WRE: Water-to-refrigerant evaporator
ARE: Air-to-refrigerant evaporator
RWC: Refrigerant-to-water condenser
EEV: Expansion valve
$T_1 - T_8$: Temperature sensor

Figure 14. Schematic of the SAASHP system [110].

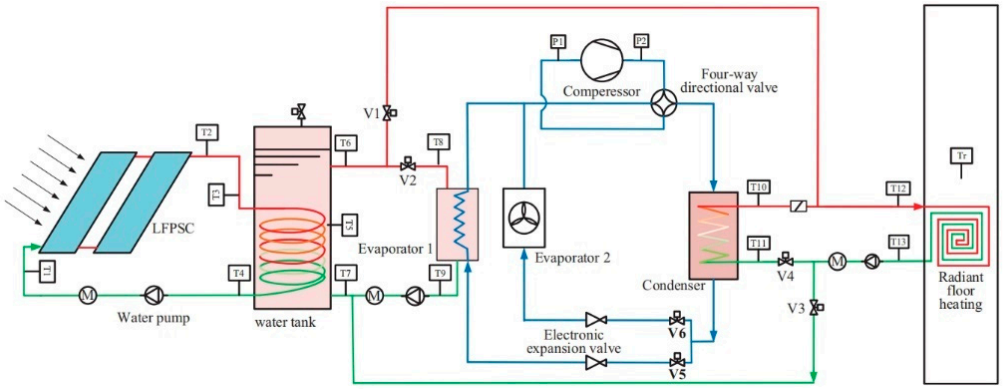

Figure 15. Schematic diagram of the LFPSC–ASHP heating system [111].

5. The Application Case of S–ASHP System

S–ASHP system has broad application prospects in the field of agriculture. In the process of agricultural production, drying is a crucial link that directly affects the quality, preservation period, and subsequent processing and utilization of agricultural products. The development of the S–ASHP system has brought a new dawn to agricultural drying operations. Kang et al. [112] designed a novel greenhouse solar-assisted heat pump drying system for drying kelp. When the drying temperature is controlled at 40 °C in an environment with an irradiance of 400 W/m^2, the system exhibits excellent performance, its COP reaches 6.810, and the kelp drying operation can be completed within 3 h. The dried kelp by this system is not only bright in color, and intact in appearance, but also rich in mannitol content, which fully demonstrates the high efficiency and superiority of this new drying system in kelp drying treatment. Thomasson et al. [113] established an experimental drying system consisting of an ASHP and a SC in Finland. Its main purpose is to dry wood biomass. The experiment lasted 316 h, which fully verified the performance indexes of the drying system. The average drying rate of this system can reach 33.0 kg/h, and the error range is 5.4 kg/h. Compared with the drying method relying solely on solar energy, the drying rate has been significantly improved. The drying rate of pure solar energy is only

9.0 kg/h, and the error range is 3.2 kg/h. In the field of hot water supply, the S–ASHP system also has a variety of specific applications. Among them, Liu et al. [114] carried out in-depth research on the solar hot air source heat pump water heater (SA–WH). The system adopts the structure of SC and ASHP in parallel. The experimental operation mode is set as follows: during the daytime, the hot water is mainly heated by the SC, and when the time comes to 18:00, the ASHP is turned on until 19:00. It is found that the system has excellent performance, which can effectively utilize the relatively insufficient solar energy resources, so as to effectively meet the energy supply and demand of domestic hot water in the transition season. In the transition season, when under 80% of the operating conditions, it shows a higher energy efficiency performance than the benchmark operating conditions, which fully demonstrates the advantages and potential of the system in heating applications. In the field of building heating, Liu et al. [115] proposed a solar-air source heat pump coupled heating system based on a heat grid (NH–SAHP). The system model is established by TRNSYS, and its control strategy is optimized and improved. During the heating season, the NH–SASHP system is more energy efficient than the ASHP system. Specifically, compared with the ASHP system, the energy-saving rate of the NH–SASHP system is as high as 50.79%. Under the most unfavorable working environment conditions, the indoor temperature compliance rate can still reach 100%, and its operating cost is only about 72.3% of the ASHP system. This series of data fully proves the high efficiency and economy of NH–SASHP system in building heating applications, and provides a valuable reference example for the development of building heating technology.

With the continuous evolution and optimization of technology, this S–ASHP system is bound to open up a new world of application in a wider range of fields. It will become a core force in the process of green transformation in many fields, effectively promote the efficient use of energy, inject strong impetus into the sustainable development of the industry, and effectively improve people's quality of life. Its potential for development is huge, which is worthy of our in-depth exploration and vision. On the road to future development, it will surely shine more brightly and lead the related fields to a new realm of environmental protection, efficiency, and sustainability.

6. Conclusions and Foresight

The S–ASHP system shows significant advantages in energy efficiency. By combing and analyzing the various architectural forms of the system, it can be found that it makes full use of the complementarity of solar energy and ASHP, and can flexibly respond to the thermal energy demand under different climatic conditions. Different architectures of the S–ASHP system can be divided into DX–S-ASHP and IDX–S-ASHP, and the IDX–S-ASHP is divided into series type, parallel type, and hybrid type. There are significant differences between the systems. The direct expansion system has good energy efficiency because the SC is directly used as an evaporator. The indirect expansion system can flexibly cope with different working conditions through independent SC and ASHPs. The series system is suitable for the environment with abundant solar energy but low temperature, and the ASHP is not enough to supplement the solar energy. The parallel system optimizes the operation, according to the state of solar energy and air sources to improve the overall performance. The hybrid system combines the advantages of both, with high flexibility and stability. The system provides flexible and diverse solutions for different application scenarios, which not only meets the needs of users but also achieves efficient use of energy.

When the S–ASHP system is employed in the heating domain, it is essential to comprehensively take into account the climatic conditions of various regions and the specific requirements of users. To start with, in regions with ample solar energy resources yet low temperatures, the DX–S-ASHP system or the Series IDX–S-ASHP system can be given priority. These systems can maximize the advantages of SC to thoroughly gather energy and ASHP to effectively make up for heat insufficiency, thus guaranteeing stable heating. In areas where solar and air source conditions are more intricate and variable, the Hybrid IDX–S-ASHP system is an excellent option. They can integrate the merits of both,

respond nimbly to different working conditions, ensure the high flexibility and stability of the heating system, and fulfill diversified heating demands. For areas with relatively minor fluctuations in energy supply, the Parallel IDX–S-ASHP system can optimize its operation based on the real-time status of solar energy and air source, and enhance the overall heating performance, thereby achieving the dual aims of efficient energy utilization and improvement of heating quality.

As the global demand for a low-carbon economy and sustainable development continues to grow, S–ASHP system technology will continue to develop and optimize. In the future, by introducing advanced technologies, such as intelligent control algorithm, artificial intelligence, and big data analysis, the utilization rate of solar energy can be further improved, the energy consumption of ASHP can be reduced, and the overall performance of the system can be improved. In the meantime, considering the climate conditions, differences in energy resources, and individual needs of users in different regions, future research should pay more attention to the regional adaptability and customized design of the system. For example, in cold regions, it is necessary to improve the cold resistance and operating efficiency of ASHP, in areas with sufficient light, more emphasis should be placed on the improvement of solar energy capture and storage capacity.

In short, the development of the S–ASHP system is not only the embodiment of technological progress but also an important path to achieve energy transformation and environmental protection. With the continuous innovation and optimization of technology, the system will occupy an increasingly important position in the global energy landscape in the future.

Author Contributions: Conceptualization, Z.L.; methodology, X.M.; writing—original draft, X.Z. All authors have read and agreed to the published version of the manuscript.

Funding: The authors are thankful for support from the Science and Technology Department of Shaanxi Province (2023-YBNY-115 and 2023-YBNY-205).

Data Availability Statement: Interested researchers can contact xinzhou0958@163.com Xin Zhou requested to obtain the data and materials used in this study.

Acknowledgments: The author would like to express his sincere thanks to the reviewers and editors for their valuable opinions and constructive suggestions.

Conflicts of Interest: The authors declare that there are no conflicts of interest regarding the publication of this article.

References

1. Tian, R.P.; Wu, D.W. China's energy consumption, energy consumption structure and economic growth. *Times Fortune* **2020**, *1*, 74.
2. Emmi, G.; Bordignon, S.; Zarrella, A.; Carli, M.D. A dynamic analysis of a SAGSHP system coupled to solar thermal collectors and photovoltaic-thermal panels under different climate conditions. *Energy Convers. Manag.* **2020**, *213*, 112851. [CrossRef]
3. Li, J.G.; Huang, J.S. The expansion of China's solar energy: Challenges and policy options. *Renew. Sustain. Energy Rev.* **2020**, *132*, 110002. [CrossRef]
4. Yang, X.J.; Hu, H.; Tan, T.; Li, J. China's renewable energy goals by 2050. *Environ. Dev.* **2016**, *20*, 83–90. [CrossRef]
5. Juaidi, A.; Anayah, F.; Assaf, R.; Hasan, A.A.; Monna, S.; Herzallah, L.; Abdallah, A.; Dutournié, P.; Jeguirim, M. An overview of renewable energy strategies and policies in Palestine: Strengths and challenges. *Energy Sustain. Dev.* **2022**, *68*, 258–272. [CrossRef]
6. Johnson, N.; McGirr, A.; Hatton, L.; Bamisile, O.; Rooney, A.R.; Staffell, I. Evaluating clean electricity transition progress across UK political pledges and G7 countries. *Energy Strategy Rev.* **2024**, *55*, 101510. [CrossRef]
7. Jayaraj, N.; Klarin, A.; Ananthram, S. The transition towards solar energy storage: A multi-level perspective. *Energy Policy* **2024**, *192*, 114209. [CrossRef]
8. Tagle, P.D.; Agraz, A.; Rivera, C.I. Study of applications of parabolic trough solar collector technology in Mexican industry. *Energy Procedia* **2016**, *91*, 661–667. [CrossRef]
9. Wu, X.; Yan, C.; Han, W.; Pan, Z. Integrated design of solar photovoltaic power generation technology and building construction based on the Internet of Things. *Alex. Eng. J.* **2022**, *61*, 2775–2786. [CrossRef]
10. Jiang, H.; Lu, N.; Yao, L.; Qin, J.; Liu, T. Impact of climate changes on the stability of solar energy: Evidence from observations and reanalysis. *Renew. Energy* **2023**, *208*, 726–736. [CrossRef]
11. Yu, S.; Su, Y.; Cai, W.; Qiu, G. Experimental investigation on an air source heat pump system with a novel anti-frosting evaporator. *Appl. Therm. Eng.* **2023**, *221*, 119910. [CrossRef]

12. Li, Z.; Wei, W.; Wang, W.; Sun, Y.; Wang, S.; Lin, Y.; Huang, C.Y.; Deng, S. Experimental study on the effects of melted frost icing on the operating performances of air source heat pump. *Appl. Therm. Eng.* **2024**, *238*, 122136. [CrossRef]
13. Kim, T.; Choi, B.I.; Han, Y.S.; Do, K.H. A comparative investigation of solar-assisted heat pumps with solar thermal collectors for a hot water supply system. *Energy Convers. Manag.* **2018**, *172*, 472–484. [CrossRef]
14. Abbasi, B.; Li, S.; Mwesigye, A. Investigation of the thermodynamic performance of a direct-expansion solar-assisted heat pump under very cold climatic conditions with and without glazing. *Int. J. Refrig.* **2024**, *158*, 329–344. [CrossRef]
15. Shi, G.H.; Aye, L.; Li, D.; Du, X.J. Recent advances in direct expansion solar assisted heat pump systems: A review. *Renew. Sustain. Energy Rev.* **2019**, *109*, 349–366. [CrossRef]
16. Zhou, J.; Zeng, C.; Wang, Z.; Lyu, W.; Tang, Y.; Wu, D.; Ji, W.; Yuan, Y. Indirect expansion solar assisted heat pump system: A review. *Sustain. Energy Technol. Assess.* **2022**, *53*, 102409. [CrossRef]
17. Suwaed, M.S.; Alturki, S.F.; Ghareeb, A.; Al-Rubaye, A.H.; Awad, O.I. Techno-economic feasibility of various types of solar collectors for solar water heating systems in hot and semi-arid climates: A case study. *Results Eng.* **2023**, *20*, 101445. [CrossRef]
18. Ma, Y.; Xi, J.F.; Cai, J.; Gu, Z.Z. TRNSYS simulation study of the operational energy characteristics of a hot water supply system for the integrated design of solar coupled air source heat pumps. *Chemosphere* **2023**, *338*, 139453. [CrossRef]
19. Gambade, J.; Noël, H.; Glouannec, P.; Magueresse, A. In-situ assessment of a solar vacuum tube collectors installation dedicated to hot water production. *Energy Rep.* **2022**, *8*, 605–615. [CrossRef]
20. Bo, R.; Fu, W.; Meng, X.; Zhang, G. Employing a fan to improve the wintery heating performance of solar air collectors with phase-change material: An experimental comparison. *Case Stud. Therm. Eng.* **2023**, *50*, 103425. [CrossRef]
21. Bogdanovics, R.; Zemitis, J.; Zajacs, A.; Borodinecs, A. Small-scale district heating system as heat storage for decentralized solar thermal collectors during non-heating period. *Energy* **2024**, *298*, 131260. [CrossRef]
22. Sathish, T.; Sivakumar, D.B.; Sivasankar, G.A.; Thilagham, K.T.; Kaliappan, S.; Saravanan, R.; Ubaidullah, M.; Tamboli, M.S.; Gupta, M. Building heating by solar parabolic through collector with metallic fined PCM for net zero energy/emission buildings. *Case Stud. Therm. Eng.* **2024**, *53*, 103862. [CrossRef]
23. Rahman, M.A.; Salahuddin, R.R.M.; Salehin, S.; Karim, M.R. Techno-economic and environmental feasibility analysis of solar industrial process heating systems in textile industries of Bangladesh. *Int. J. Thermofluids* **2023**, *20*, 100459. [CrossRef]
24. Sahoo, N.; Kumar, A. Potential assessment of solar industrial process heating and CO_2 emission reduction for Indian cement industry. *Sol. Compass* **2023**, *8*, 100064. [CrossRef]
25. Bellos, E.; Arabkoohsar, A.; Lykas, P.; Sammoutos, C.; Kitsopoulou, A.; Tzivanidis, C. Investigation of a solar-driven absorption heat transformer with various collector types for industrial process heating. *Appl. Therm. Eng.* **2024**, *244*, 122665. [CrossRef]
26. Mamani-Benito, O.; Rojas-Zegarra, M.E.; Esteban, R.F.C.; Caycho-Rodríguez, T.; Vilca, L.W.; Lingán-Huamán, S.K. New psychometric evidence for the thesis advisor abuse scale (EMAT) in Peruvian university students based on classic and modern procedures. *Heliyon* **2024**, *10*, e28475. [CrossRef]
27. Barone, G.; Buonomano, A.; Kalogirou, S.; Ktistis, P.; Palombo, A. A holistic methodology for designing novel flat plate evacuated solar thermal collectors: Modelling and experimental assessment. *Renew. Energy* **2024**, *232*, 120967. [CrossRef]
28. NematpourKeshteli, A.; Iasiello, M.; Langella, G.; Bianco, N. Using metal foam and nanoparticle additives with different fin shapes for PCM-based thermal storage in flat plate solar collectors. *Therm. Sci. Eng. Prog.* **2024**, *49*, 102690. [CrossRef]
29. Farghaly, M.B.; Alahmadi, R.N.; Sarhan, H.H.; Abdelghany, E.S. Experimental study of simultaneous effect of evacuated tube collectors coupled with parabolic reflectors on traditional single slope solar still efficiency. *Case Stud. Therm. Eng.* **2023**, *49*, 103304. [CrossRef]
30. Said, S.; Mellouli, S.; Alqahtani, T.; Algarni, S.; Ajjel, R.; Alshammari, B.M.; Kolsi, L. Performance Enhancement of Evacuated U-Tube Solar Collector integrated with Phase Change Material. *Case Stud. Therm. Eng.* **2024**, *61*, 104948. [CrossRef]
31. Rodríguez-Muñoz, J.M.; Bove, I.; Alonso-Suárez, R. Improving the experimental estimation of the incident angle modifier of evacuated tube solar collectors with heat pipes. *Renew. Energy* **2024**, *235*, 121240. [CrossRef]
32. Xiao, G.; Nie, J.; Xu, H.R.; Zhang, C.L.; Zhu, P.W. Performance analysis of a solar power tower plant integrated with trough collectors. *Appl. Therm. Eng.* **2022**, *214*, 118853. [CrossRef]
33. Chen, J.L.; Xiao, G.; Xu, H.R.; Zhou, X.; Yang, J.M.; Ni, M.J.; Cen, K.F. Experiment and dynamic simulation of a solar tower collector system for power generation. *Renew. Energy* **2022**, *196*, 946–958. [CrossRef]
34. Aseri, T.K.; Sharma, C.; Kandpal, T.C. A techno-economic appraisal of parabolic trough collector and central tower receiver based solar thermal power plants in India: Effect of nominal capacity and hours of thermal energy storage. *J. Energy Storage* **2022**, *48*, 103976. [CrossRef]
35. Wang, L.J.; Lou, J.W.; Wang, H.B.; Liu, X.R. The analysis of the development and research status of heat pump system. *Sichuan Build. Mater.* **2022**, *48*, 33–34+38.
36. Zhang, Q.L.; Zhang, L.; Nie, J.Z.; Li, Y.L. Techno-economic analysis of air source heat pump applied for space heating in northern China. *Appl. Energy* **2017**, *207*, 533–542. [CrossRef]
37. Latorre-Biel, J.I.; Jiménez, E.; García, J.L.; Martínez, E.; Jiménez, E.; Blanco, J. Replacement of electric resistive space heating by an air-source heat pump in a residential application. Environmental amortization. *Build. Env.* **2018**, *141*, 193–205. [CrossRef]
38. Chen, X.Y.; Li, Z.Q.; Dai, L.K.; Zeng, W.M.; Liu, Z.L.; Liu, M. Characteristics of intermittent heating by air source heat pump in rural areas of northern China based on indoor temperature effective guarantee rate. *J. Build. Eng.* **2024**, *95*, 110196. [CrossRef]

39. Sun, S.J.; Guo, H.; Lu, D.; Bai, Y.; Gong, M.Q. Performance of a single-stage recuperative high-temperature air source heat pump. *Appl. Therm. Eng.* **2021**, *193*, 116969. [CrossRef]
40. Sun, Y.Y.; Chen, X.; Wu, S.J.; Wei, W.Z.; Wang, W.; Deng, S.M. Performance analysis of air source heat pump space heating system with an adaptive control for supply water temperature. *Appl. Therm. Eng.* **2022**, *211*, 118401. [CrossRef]
41. Wu, D.; Jiang, J.T.; Hu, B.; Wang, R.Z.; Sun, Y. Experimental investigation and industrial application of a cascade air-source high temperature heat pump. *Renew. Energy* **2024**, *232*, 121094. [CrossRef]
42. Jordan, R.C.; Thekreld, J.L. Design and economics of solar energy heat pump systems. *Heat. Pip. Air Cond.* **1954**, *26*, 122–130.
43. Jordan, R.C.; Thekreld, J.L. Solar energy availability for heating in the United States. *Heat. Pip. Air Cond.* **1953**, *25*, 116.
44. Rong, W.L.; Xu, S.X.; Ma, G.Y.; Dai, W. Experimental study on direct expansion solar air source heat pump heating. *Refrig. Air Cond.* **2022**, *36*, 243–248.
45. Dong, X.; Tian, Q.; Li, Z. Experimental investigation on heating performance of solar integrated air source heat pump. *Appl. Therm. Eng.* **2017**, *123*, 1013–1020. [CrossRef]
46. Ran, S.Y.; Lyu, W.H.; Li, X.T.; Xu, W.; Wang, B.L. A solar-air source heat pump with thermosiphon to efficiently utilize solar energy. *J. Build. Eng.* **2020**, *31*, 101330. [CrossRef]
47. Ma, K.R.; Li, X.F.; Li, S.Q.; Gao, C.J. Contrastive research of heating performance of direct expansion solar/air assisted heat pump system and air-source heat pump. *CIESC J.* **2020**, *71* (Suppl. S1), 375–381.
48. Chinnasamy, S.; Arunachalam, A. Experimental investigation on direct expansion solar-air source heat pump for water heating application. *Renew. Energy* **2023**, *202*, 222–233. [CrossRef]
49. Jiang, Y.; Zhang, H.; Zhao, R.; Wang, Y.R.; Liu, M.Z.; You, S.J.; Wu, Z.X.; Liu, Z.K.; Wei, S. Energy, exergy, economic and environmental assessment of the triangular solar collector assisted heat pump. *Sol. Energy* **2022**, *236*, 280–293. [CrossRef]
50. Jiang, Y.; Zhang, H.; Wang, Y.M.; Wang, Y.R.; Liu, M.Z.; You, S.J.; Wu, Z.X.; Fan, M.; Wei, S. Research on the operation strategies of the solar assisted heat pump with triangular solar air collector. *Energy* **2022**, *246*, 123398. [CrossRef]
51. Song, Z.Y.; Ji, J.; Zhang, Y.Z.; Cai, J.Y.; Li, Z.M. Research on the multifunction concentrated solar-air heat pump system. *Renew. Energy* **2022**, *198*, 679–694. [CrossRef]
52. Fernández-Seara, J.; Piñeiro, C.; Dopazo, J.A.; Fernandes, F.; Sousa, P.X. Experimental analysis of a direct expansion solar assisted heat pump with integral storage tank for domestic water heating under zero solar radiation conditions. *Energy Convers. Manag.* **2012**, *59*, 1–8. [CrossRef]
53. Song, Z.Y.; Ji, J.; Li, Z.M. Comparison analyses of three photovoltaic solar-assisted heat pumps based on different concentrators. *Energy Build.* **2021**, *251*, 111348. [CrossRef]
54. Cao, Y.; Mihardjo, L.W.W.; Parikhani, T. Thermal performance, parametric analysis, and multi-objective optimization of a direct-expansion solar-assisted heat pump water heater using NSGA-II and decision makings. *Appl. Therm. Eng.* **2020**, *181*, 115892. [CrossRef]
55. Dai, H.; Xu, S.X.; Zhang, H.Y.; Ma, G.Y.; Xue, J. Simulation research on performance of direct expansion solar air-source heat pump in full working conditions. *Chin. J. Refrig. Technol.* **2022**, *42*, 21–27.
56. Fang, L. Performance analysis of direct expansion solar air sourceheat pump water heater. *Build. Energy Environ.* **2020**, *39*, 7–11.
57. Cai, J.Y.; Li, Z.H.; Ji, J.; Zhou, F. Performance analysis of a novel air source hybrid solar assisted heat pump. *Renew. Energy* **2019**, *139*, 1133–1145. [CrossRef]
58. Yu, X.H.; Wang, T.; Gao, Z. Performance analysis of evacuated tube direct expansion solar heat pump system. *Acta Energiae Solaris Sin.* **2023**, *44*, 166–173.
59. Li, Z.Q.; Huang, X.H. Simulation analysis on operation performance of a hybrid heat pump system integrating photovoltaic/thermal and air source. *Appl. Therm. Eng.* **2022**, *200*, 117693. [CrossRef]
60. Liu, Z.J.; Wang, Q.M.; Wu, D.; Zhang, Y.L.; Yin, H.; Yu, H.C.; Jin, G.Y.; Zhao, X.D. Operating performance of a solar/air-dual source heat pump system under various refrigerant flow rates and distributions. *Appl. Therm. Eng.* **2020**, *178*, 115631. [CrossRef]
61. Cai, J.Y.; Zhou, H.H.; Xu, L.J.; Shi, Z.R.; Zhang, T. Performance optimization of solar-air composite source multi-functional heat pump with different control schemes. *Sustain. Energy Technol. Assess.* **2022**, *50*, 101803. [CrossRef]
62. Kong, X.Q.; Li, J.X.; Li, Y. Performance Analysis of Three Different Refrigerants in a Direct-expansion Solar-Assisted Heat Pump Water Heater. *J. Shanghai Jiaotong Univ.* **2016**, *50*, 506.
63. Yang, H.; Wang, X.Y.; Yao, S. Thermodynamic analysis of a novel solar photovoltaic thermal collector coupled with switchable air source heat pump system. *Appl. Therm. Eng.* **2023**, *218*, 119410. [CrossRef]
64. Cai, J.Y.; Ji, J.; Wang, Y.Y.; Huang, W.Z. Numerical simulation and experimental validation of indirect expansion solar-assisted multi-functional heat pump. *Renew. Energy* **2016**, *93*, 280–290. [CrossRef]
65. Cai, J.Y.; Zhang, F.; Ji, J. Comparative analysis of solar-air dual source heat pump system with different heat source configurations. *Renew. Energy* **2020**, *150*, 191–203. [CrossRef]
66. Liu, Z.J.; Jia, C.X.; Li, Z.; Li, A.S.; Li, C.L.; Chen, L. A solar-assisted air source heat pump equipment. *Build. Energy Effic.* **2018**, *46*, 44–48.
67. Du, X. Solar Air Source Heat Pump Coupled Heating System Evaluation System Investigation. Master's Thesis, Beijing University of Civil Engineering and Architecture, Beijing, China, 2022.
68. Xie, L.Y.; Zhuang, D.; Ding, G. Measurement and correlation development of the diffusion coefficient of R32 in lubricating oil. *Int. J. Refrig.* **2024**, *162*, 179–193. [CrossRef]

69. Yue, B.; Li, G.; Li, J.F.; Wu, Z.G.; Zhang, H.; Shao, Y.P.; Zhuang, D.W.; Ding, G.L.; Weng, X.M.; Zhou, Z. Flow condensation heat transfer correlation development of R32-oil mixture inside a micro-fin tube. *Int. J. Refrig.* **2024**, *159*, 176–184. [CrossRef]
70. Li, G.; Zhuang, D.W.; Xie, L.Y.; Ding, G.L.; Yue, B.; Fan, B.; Zhang, H.; Shao, Y.P. Development of boiling flow pattern map and heat transfer correlation of R32-oil mixture inside a horizontal micro-fin tube. *Int. J. Refrig.* **2023**, *155*, 320–332. [CrossRef]
71. Wei, M.; Ding, C.; Rosenquist, G.; Coughlin, K.; Cubero, E.; Burke, T.; Abdelaziz, O. Benefits and challenges in deployment of low global warming potential R290 refrigerant for room air conditioning equipment in California. *Sustain. Energy Technol. Assess.* **2024**, *70*, 103937. [CrossRef]
72. Piechnik, E.; Palacz, M.; Tolstorebrov, I.; Bodys, J.; Smolka, J.; Haida, M.; Eikevik, T.M. Design and evaluation of an R290-based freezing system and air distribution in a domestic-scale microwave-heated freeze-dryer prototype. *Innov. Food Sci. Emerg. Technol.* **2024**, *96*, 103781. [CrossRef]
73. Zhao, Y.; Du, Y.J.; Lin, J.; Guo, N.N.; Wu, J.H. Start-up characteristics of a R290 rotary compressor for an air source heat pump under low ambient temperature condition. *Int. J. Refrig.* **2024**, *159*, 385–394. [CrossRef]
74. Gullo, P.; Birkelund, M.; Kriezi, E.E.; Kærn, M.R. Comprehensive experimental performance study on a small-capacity transcritical R744 vapour-compression refrigeration unit equipped with an innovative ejector. *Int. J. Refrig.* **2023**, *152*, 192–203. [CrossRef]
75. Pardiñas, Á.Á.; Selvnes, H.; Banasiak, K.; Hafner, A. Next generation of ejector-supported R744 booster systems for commercial refrigeration at all climates. *Int. J. Refrig.* **2023**, *148*, 168–178. [CrossRef]
76. Fabris, F.; Pardiñas, Á.Á.; Marinetti, S.; Rossetti, A.; Hafner, A.; Minetto, S. A novel R744 multi-temperature cycle for refrigerated transport applications with low-temperature ejector: Experimental ejector characterization and thermodynamic cycle assessment. *Int. J. Refrig.* **2023**, *152*, 26–35. [CrossRef]
77. Qin, Y.B.; Li, N.X.; Zhang, H.; Liu, B.L. A thermodynamic analysis of the Linde-Hampson cycle using low-GWP R1234yf-blends. *Case Stud. Therm. Eng.* **2023**, *49*, 103358. [CrossRef]
78. Daisuke, J.; Mikajiri, N.; Nobunaga, M.; Inoue, N. Condensation heat transfer of pure refrigerants R1234yf and R32 inside multiple circular minichannels. *Int. J. Heat Mass Transf.* **2022**, *195*, 123146.
79. Kemprai, P.P.; Murthy, K.V.R.; Ranganayakulu, C.; Muthukumar, P. Experimental investigation on condensation heat transfer coefficient and frictional pressure drop of low GWP refrigerant R1234yf on a wavy fin surface. *Therm. Sci. Eng. Prog.* **2024**, *47*, 102300. [CrossRef]
80. Chen, X.X.; Ding, T.; Wang, X.Y.; Li, Z. Research on energy saving potentials using pure and zeotropic refrigerants in data center cooling systems. *Case Stud. Therm. Eng.* **2024**, *57*, 104324. [CrossRef]
81. Sieres, J.; Ortega, I.; Cerdeira, F.; Alvarez, E. Influence of the refrigerant charge in an R407C liquid-to-water heat pump for space heating and domestic hot water production. *Int. J. Refrig.* **2020**, *110*, 28–37. [CrossRef]
82. Dione, K.R.; Louahlia, H.; Marion, M.; Berçaits, J.L. Evaporation heat transfer and pressure drop for geothermal heat pumps working with refrigerants R134a and R407C. *Int. Commun. Heat Mass Transf.* **2018**, *93*, 1–10. [CrossRef]
83. Bellos, E.; Tzivanidis, C. Multi-objective optimization of a solar assisted heat pump-driven by hybrid PV. *Appl. Therm. Eng.* **2019**, *149*, 528–535. [CrossRef]
84. Wang, Q.; Liu, Y.Q.; Liang, G.F.; Li, J.R.; Sun, S.F.; Chen, G.M. Development and experimental validation of a novel indirect-expansion solar-assisted multifunctional heat pump. *Energy Build.* **2011**, *43*, 300–304. [CrossRef]
85. Long, J.B.; Zhang, R.C.; Lu, J.; Xu, F. Heat transfer performance of an integrated solar-air source heat pump evaporator. *Energy Convers. Manag.* **2019**, *184*, 626–635. [CrossRef]
86. Liu, Y.; Zhou, G.H.; Ma, J. Experimental Study of a Solar Assisted Air Source Heat Pump in Heating Condition. *Adv. Mater. Res.* **2011**, *243*, 4909–4912. [CrossRef]
87. Wang, Q.Q.; Wang, F.; Liu, D.H.; Wang, Y.X.; He, Z.H. Research on heating characteristics of solar assisted air-source heat pump composite system. *Agric. Equip. Veh. Eng.* **2021**, *59*, 50–54.
88. Liu, Y.X. Research on Optimal Design of Solar Assisted Lowtemperature Air-Source Heat Pump Heating Systemin a Railway Station Building. Master's Thesis, Huazhong University of Science and Technology, Wuhan, China, 2018.
89. Hu, Y.; Cheng, Z.J.; Cui, L. Design of variable frequency light-heat-air source heat pump system based on particle swarm optimization. *Renew. Energy Resour.* **2022**, *40*, 866–873.
90. Liu, Z.Q.; Jiang, Z.S.; Huang, G.H.; Ye, X.P.; You, Z.P.; Li, P.Y. Research on energy saving strategy of solar-assisted heat pump hot water system. *Energy Eng.* **2017**, *01*, 43–46+53.
91. Lu, T.; Liu, X.F.; Chen, W.J.; Jiang, H.H. Dynamic Optimization of Solar Coupled Heat Pump Hot Water System Control Strategy. *Build. Energy Effic.* **2022**, *50*, 98–104.
92. Ma, Y.C.; Xi, J.F.; Cai, J.; Gu, Z.Z. The optimization and energy efficiency analysis of a multi-tank solar-assisted air source heat pump water heating system. *Therm. Sci. Eng. Prog.* **2024**, *48*, 102387. [CrossRef]
93. Zhang, T.H.; Wang, F.X.; Gao, Y.; Liu, Y.J.; Guo, Q.; Zhao, Q.X. Optimization of a solar-air source heat pump system in the high-cold and high-altitude area of China. *Energy* **2023**, *268*, 126653. [CrossRef]
94. Zheng, Z.H.; Zhou, J.; Xu, F.; Deng, G. Solar assisted air source heat pump systems for campus water heating in China: Economic optimization of solar fraction design. *Appl. Therm. Eng.* **2022**, *213*, 118767. [CrossRef]
95. Wu, J.; Kang, Y.; Feng, J. Modeling and Optimization of Solar Collector Design for the Improvement of Solar-Air Source Heat Pump Building Heating System. *Energy Eng.* **2023**, *120*, 2783–2802. [CrossRef]

96. Long, T.H.; Qiao, Z.Y.; Wang, M.L.; Li, Y.; Lu, J.C.; Li, W.Y.; Zeng, L.Y.; Huang, S. Performance analysis and optimization of a solar-air source heat pump heating system in Tibet, China. *Energy Build.* **2020**, *220*, 110084. [CrossRef]
97. Xu, L.N.; Li, M.; Zhang, Y.; Luo, X. Applicability and comparison of solar-air source heat pump systems between cold and warm regions of plateau by transient simulation and experiment. *Build. Simul.* **2021**, *14*, 1697–1708. [CrossRef]
98. Liu, Y.F.; Mu, T.; Luo, X.; Hu, X.X.; Hu, D.Z. Equipment capacity and heating network pipe diameter optimization of centralized solar heating system in areas abundant with solar energy resources. *Acta Energiae Solaris Sin.* **2023**, *44*, 85–93.
99. Wang, Y.; Gao, W.X.; Zhou, W.Y.; Yang, L.; Wang, Q. Study on performances of heating system with solar hybrid air source heat pump in winter. In Proceedings of the IOP Conference Series: Materials Science and Engineering, Suzhou, China, 22–24 June 2018.
100. Liu, Z.J.; Liu, Y.W.; Wu, D.; Jin, G.Y.; Yu, H.C.; Ma, W.S. Performance and feasibility study of solar-air source pump systems for low-energy residential buildings in Alpine regions. *J. Clean. Prod.* **2020**, *256*, 120735. [CrossRef]
101. Li, X.L.; Wang, X.; Wang, Y.L. Experimental study of coupled solar and air source heat pump heating system. In *Journal of Physics: Conference Series*; IOP Publishing: Bristol, UK, 2023.
102. Hou, F.; He, T.; Lu, Y.; Sun, H.C.; Li, Y.W.; Yuan, P. Experimental and Simulation study on the performance of a solar assisted multi-source heat pump drying system in Zhengzhou area. *Renew. Energy* **2024**, *229*, 120771. [CrossRef]
103. Yu, T.; Zhang, L.L.; Chu, G.M. Analysis and optimization of the solar hot water heating system assisted by air source heat pump. *J. Shandong Jianzhu Univ.* **2021**, *36*, 27–34.
104. Huan, C.; Li, S.T.; Wang, F.H.; Liu, L.; Zhao, Y.J.; Wang, Z.H.; Tao, P.F. Performance analysis of a combined solar-assisted heat pump heating system in Xi'an, China. *Energies* **2019**, *12*, 2515. [CrossRef]
105. Yang, L.W.; Hua, N.; Pu, J.H.; Xia, Y.; Zhou, W.B.; Xu, R.J.; Yang, T.; Belyayev, Y.; Wang, H.S. Analysis of operation performance of three indirect expansion solar assisted air source heat pumps for domestic heating. *Energy Convers. Manag.* **2022**, *252*, 115061. [CrossRef]
106. Yang, L.W.; Li, Y.; Yang, T.; Wang, H.S. Low temperature heating operation performance of a domestic heating system based on indirect expansion solar assisted air source heat pump. *Sol. Energy* **2022**, *244*, 134–154. [CrossRef]
107. Gong, J.B. Study on Operation Characteristics and Optimal Control of Solar-Air Double Heat Source Composite Heat Pump System. Master's Thesis, Hebei University of Engineering, Handan, China, 2021.
108. Wang, L.; Fu, W.X.; Tan, Y.Y.; Liang, K.F.; Yuan, J.F. Research on heating performance of solar assisted dual-source hybrid heat pump systems. *Acta Energiae Solaris Sin.* **2019**, *40*, 2272–2278.
109. Li, J.P.; Wei, S.F.; Dong, Y.H.; Liu, X.M.; Novakovic, V. Technical and economic performance study on winter heating system of air source heat pump assisted solar evacuated tube water heater. *Appl. Therm. Eng.* **2023**, *221*, 119851. [CrossRef]
110. Yang, L.W.; Xu, R.J.; Zhou, W.B.; Li, Y.; Yang, T.; Wang, H.S. Investigation of solar assisted air source heat pump heating system integrating compound parabolic concentrator-capillary tube solar collectors. *Energy Convers. Manag.* **2023**, *277*, 116607. [CrossRef]
111. Li, J.P.; Qu, C.F.; Li, C.J.; Liu, X.M.; Novakovic, V. Technical and economic performance analysis of large flat plate solar collector coupled air source heat pump heating system. *Energy Build.* **2022**, *277*, 112564. [CrossRef]
112. Kang, H.; Zhang, G.; Mu, G. Design of a greenhouse solar-assisted heat pump dryer for kelp (Laminaria japonica): System performance and drying kinetics. *Foods* **2022**, *11*, 3509. [CrossRef]
113. Thomasson, T.; Raitila, J.; Tsupari, E. Experimental and techno-economic analysis of solar-assisted heat pump drying of biomass. *Energy Rep.* **2024**, *11*, 316–326. [CrossRef]
114. Liu, M.; He, Y.; Zhang, H.; Su, H.; Zhang, Z. The feasibility of solar thermal-air source heat pump water heaters in renewable energy shortage regions. *Energy* **2020**, *197*, 117189. [CrossRef]
115. Liu, X.; Wang, X.; Chuang, E.; Huang, K.; Feng, G.; Li, X.; Cui, Y. Research on solar-air source heat pump coupled heating system based on heat network in severe cold regions of China. *Energy Built Env.* **2024**, *08*, 008. [CrossRef]

Disclaimer/Publisher's Note: The statements, opinions and data contained in all publications are solely those of the individual author(s) and contributor(s) and not of MDPI and/or the editor(s). MDPI and/or the editor(s) disclaim responsibility for any injury to people or property resulting from any ideas, methods, instructions or products referred to in the content.